Inactive

NACA

RESEARCH MEMORANDUM

for the

Bureau of Aeronautics, Department of the Navy

EFFECT OF VARIOUS MODIFICATIONS ON DRAG AND LONGITUDINAL

STABILITY AND CONTROL CHARACTERISTICS AT TRANSONIC

SPEEDS OF A MODEL OF THE XF7U-1 TAILLESS AIRPLANE

NACA WING-FLOW METHOD

TED NO. NACA DE 307

By Richard H. Sawyer and James P. Trant, Jr.

Langley Aeronautical Laboratory
Langley Air Force Base, Va.

NATIONAL ADVISORY COMMITTEE
FOR AERONAUTICS
WASHINGTON
APR 20 1950

NACA RM SL50D18

NATIONAL ADVISORY COMMITTEE FOR AERONAUTICS

RESEARCH MEMORANDUM

for the

Bureau of Aeronautics, Department of the Navy

EFFECT OF VARIOUS MODIFICATIONS ON DRAG AND LONGITUDINAL

STABILITY AND CONTROL CHARACTERISTICS AT TRANSONIC

SPEEDS OF A MODEL OF THE XF7U-1 TAILLESS AIRPLANE

NACA WING-FLOW METHOD

TED NO. NACA DE 307

By Richard H. Sawyer and James P. Trant, Jr.

SUMMARY

An investigation was made by the NACA wing-flow method to determine the drag, pitching-moment, lift, and angle-of-attack characteristics at transonic speeds of various configurations of a semispan model of an early configuration of the XF7U-1 tailless airplane. The results of the tests indicated that for the basic configuration with undeflected ailavator, the zero-lift drag rise occurred at a Mach number of about 0.85 and that about a five-fold increase in drag occurred through the transonic speed range. The results of the tests also indicated that the drag increment produced by -8.0° deflection of the ailavator increased with increase in normal-force coefficient and was smaller at speeds above than at speeds below the drag rise. The drag increment produced by 35° deflection of the speed brakes varied from 0.040 to 0.074 depending on the normal-force coefficient and Mach number. These values correspond to drag coefficients of about 0.40 and 0.75 based on speed-brake frontal area. Removal of the fin produced a small positive drag increment at a given normal-force coefficient at speeds during the drag rise. A large forward shift of the neutral-point location occurred at Mach numbers above about 0.90 upon removal of the fin, and also a considerable forward shift throughout the Mach number range occurred upon deflection of the speed brakes. Ailavator ineffectiveness or reversal at low deflections, similar to that determined in previous tests of the basic configuration of the model in the Mach

number range from about 0.93 to 1.0, was found for the fin-off configuration and for the model equipped with skewed (more highly sweptback) hinge-line ailavators. With the speed brakes deflected, little or no loss in the incremental pitching moment produced by deflection of the ailavator from $0°$ to $-8.0°$ occurred in the Mach number range from 0.85 to 1.0 in contrast to a considerable loss found in previous tests with the speed brakes off.

INTRODUCTION

As a part of the investigation of the aerodynamic characteristics of complete airplane configurations in the transonic speed range, tests have been made by the NACA wing-flow method on a 0.026-scale semispan model of an early configuration of the Chance Vought XF7U-1 airplane. The results of an investigation of the longitudinal stability and control characteristics of the basic configuration of the model have been reported in reference 1. The present paper presents the results of normal-force, pitching-moment, and angle-of-attack measurements at various ailavator settings for the model with the fin removed and for the model equipped with speed brakes. Pitching-moment measurements are also presented at several ailavator deflections for the model equipped with an ailavator having a skewed (more highly sweptback) hinge line. Results of drag measurements are given for the basic configuration of the model with the original ailavator deflected $0°$ and $-8°$, the model with the fin removed, and the model equipped with speed brakes deflected $35°$. The tests covered a Mach number range from about 0.65 to 1.10.

SYMBOLS

q   effective dynamic pressure

S   wing area of model

b   twice wing span of model

$\bar{c}$ mean aerodynamic chord of model

C_N normal-force coefficient $\left(\dfrac{\text{Normal force}}{qS}\right)$

C_M pitching-moment coefficient referred to $0.17\bar{c}$
$\left(\dfrac{\text{Pitching moment}}{qS\bar{c}}\right)$

C_D drag coefficient $\left(\dfrac{\text{Drag}}{qS}\right)$

ΔC_D increment in drag coefficient

α angle of attack

δ_a deflection of ailavator (measured in plane normal to Y-axis of model)

M effective Mach number

$\dfrac{\partial C_N}{\partial \alpha}$ slope of normal-force curve per degree

$\dfrac{\partial C_M}{\partial C_N}$ slope of pitching-moment curve

n.p.   neutral-point location, percent $\bar{c}$ $\left(-100\dfrac{\partial C_M}{\partial C_N} + 17\right)$

R Reynolds number based on $\bar{c}$

APPARATUS AND TESTS

The tests were made by the NACA wing-flow method in which the model is mounted in the high-speed flow over the wing of an F-51D airplane.

Photographs of the 0.026-scale model equipped with an end plate at the fuselage center line are given as figures 1 and 2. A detailed three-view drawing is shown in figure 3. The geometric characteristics of the model are given in table I, which also includes the dimensions of the full-scale airplane for comparison. The model was originally equipped with five interchangeable ailavators having fixed deflections of $0°$, $-1.6°$, $-4.9°$, $-8.0°$, and $-13.2°$ measured in a plane normal to the Y-axis of the model. The hinge line of the original ailavators was swept back $24.5°$. Additional ailavators having a skewed (sweptback $35°$) hinge line (see fig. 3) were constructed with fixed deflections of $-4.6°$ and $-11.2°$. Details of the upper- and lower-surface speed brakes are given in figure 3. The speed brakes were wedge-shaped blocks designed to simulate $35°$ deflection of the actual speed brakes. The model was also equipped with a fillet, shaped to the wing contour, which filled the gap left in the wing on removal of the fin. The model was mounted on a shank which

passed through a slot in the airplane wing and was supported on a strain-
gage balance. The model and balance were arranged to rotate as a unit;
therefore, the balance measured the forces normal and parallel to the
chord line of the model. A free-floating vane, shown in figure 2, was
used to determine the direction of air flow at the model location.

The chordwise and vertical gradients of velocity over the F-51D air-
plane wing in the region of the model were similar to those of the tests
of reference 2. The effective Mach number M and the effective dynamic
pressure q were determined by integrating their distributions over the
area covered by the wing of the model.

Tests of the model with the fin removed were made with the original
ailavators having deflections of 0°, -4.9°, and -8.0°. The model was
also tested with the fin on with the skewed-hinge-line ailavators of
-4.6° and -11.2° deflection. Additional tests were made with the fin on
and with the speed brakes both installed and off with the original aila-
vators having deflections of 0° and -8.0°. The tests were made by con-
tinuously oscillating the model through an angle-of-attack range of about
-5° to 15° at about 20° per second during the high-speed flight of the
F-51D airplane. Measurements were also made at fixed angles of attack
of about 0° and 10° on the basic configuration with the model separated
from, but in the presence of, the end plate which was fixed to the sur-
face of the F-51D airplane wing. The gap between the fuselage and the
end plate was approximately 0.007 inch. The end-plate effects determined
in the tests with the model separated from, but in the presence of, the
end plate were found to be negligible and hence no corrections for the
end plate were applied to the results presented. Also, no measurements
were made of the effects of the inlet-velocity ratio of the duct (see
fig. 3) on the results presented.

Two flight-test procedures were followed in relation to the Reynolds
number and Mach number ranges covered by the tests. In one procedure,
three runs were made: a dive from high altitude, a dive from medium alti-
tude, and a low-altitude, high-speed, level-flight run. Three ranges of
Reynolds number were thus obtained for the range of Mach numbers covered.
(See fig. 4.) In the other procedure, the tests were made by diving to
a medium altitude and continuing the dive within the placard limits of
the airplane to a low altitude where a pull-out and deceleration to low
speed was effected. This maneuver gave the maximum Reynolds number at a
given Mach number attainable within the placard limits of the airplane
(fig. 4).

Typical examples of the pitching-moment, angle-of-attack, and drag
data at zero normal-force coefficient as obtained in the tests at three
altitudes are given in figure 5. The large amount of hysteresis evident
for the angle-of-attack data was caused by unequal amounts of electrical
damping in the normal-force and angle-of-attack recording circuits.

PRESENTATION OF RESULTS

The results presented are summarized in tabular form as follows:

Figure	Configuration	Results
6(a)	Basic, $\delta_a = 0^\circ$	C_D against M at $C_N = K$
6(b)	Basic, $\delta_a = -8.0^\circ$	C_D against M at $C_N = K$
6(c)	Speed brakes on, $\delta_a = 0^\circ$	C_D against M at $C_N = K$
7(a)	Fin off, $\delta_a = 0^\circ$	C_M and α against M at $C_N = K$
7(b)	Fin off, $\delta_a = -4.9^\circ$	C_M and α against M at $C_N = K$
7(c)	Fin off, $\delta_a = -8.0^\circ$	C_M and α against M at $C_N = K$
8(a)	Speed brakes on, $\delta_a = 0^\circ$	C_M and α against M at $C_N = K$
8(b)	Speed brakes on, $\delta_a = -8.0^\circ$	C_M and α against M at $C_N = K$
9	Skewed ailavators, $\delta_a = 0^\circ$, -4.6°, -11.2°	C_M against M at $C_N = K$
10(a)	Basic, $\delta_a = 0^\circ$	C_D against C_N at $M = K$
10(b)	Basic, $\delta_a = -8.0^\circ$	C_D against C_N at $M = K$
10(c)	Speed brakes on, $\delta_a = 0^\circ$	C_D against C_N at $M = K$
11(a)	Basic, $\delta_a = -8.0^\circ$ minus basic, $\delta_a = 0^\circ$	ΔC_D against M at $C_N = K$
11(b)	Speed brakes on, $\delta_a = 0^\circ$ minus basic, $\delta_a = 0^\circ$	ΔC_D against M at $C_N = K$
11(c)	Fin off, $\delta_a = 0^\circ$ minus basic, $\delta_a = 0^\circ$	ΔC_D against M at $C_N = K$
12	Fin off, $\delta_a = 0^\circ$, -4.9°, -8.0°	C_N against α at $M = K$
13	Speed brakes on, $\delta_a = 0^\circ$, -8.0°	C_N against α at $M = K$
14	Fin off, $\delta_a = 0^\circ$, -4.9°, -8.0°	$\partial C_N / \partial \alpha$ against M
15	Speed brakes on, $\delta_a = 0^\circ$, -8.0°	$\partial C_N / \partial \alpha$ against M
16(a)	Fin off, $\delta_a = 0^\circ$	C_M against C_N at $M = K$
16(b)	Fin off, $\delta_a = -4.9^\circ$	C_M against C_N at $M = K$
16(c)	Fin off, $\delta_a = -8.0^\circ$	C_M against C_N at $M = K$
17(a)	Speed brakes on, $\delta_a = 0^\circ$	C_M against C_N at $M = K$
17(b)	Speed brakes on, $\delta_a = -8.0^\circ$	C_M against C_N at $M = K$
18	Fin off, $\delta_a = 0^\circ$, -4.9°, -8.0°	$\partial C_M / \partial C_N$ against M
19	Speed brakes on, $\delta_a = 0^\circ$, -8.0°	$\partial C_M / \partial C_N$ against M
20	Fin off, $\delta_a = 0^\circ$, -4.9°, -8.0°	C_M against M at $C_N = K$
21	Speed brakes on, $\delta_a = 0^\circ$, -8.0°	C_M against M at $C_N = K$
22	Skewed ailavators, $\delta_a = 0^\circ$, -4.6°, -11.2°	C_M against M at $C_N = K$

The pitching-moment results presented in figure 9 for the model equipped with the skewed-hinge-line ailavators also include the results of the present tests of the basic configuration with undeflected aila- vator since these measurements resulted in pitching moments somewhat different from those presented in reference 1 and are believed to be more suitable for comparison with the skewed-hinge-line-ailavator results. The results shown in figure 11(c) for the configuration with the fin removed were obtained from fin-on and fin-off results (not presented), whose absolute magnitude was approximately 0.01 drag coefficient higher than results previously attained; however, the incremental drag results presented are considered to be of value. The normal-force-curve slopes $\partial C_N / \partial \alpha$ given in figures 14 and 15 were taken over the linear portion of the curves presented in figures 12 and 13. The pitching-moment-curve slopes shown in figures 18 and 19 were taken as the tangent to the curves (figs. 16 and 17) at the normal-force coefficient (also shown in figs. 18 and 19) required for level flight at 30,000 feet altitude with a wing loading of 28. Comparative results taken from reference 1 are presented in figures 12 to 22.

DISCUSSION OF RESULTS

Drag Results

The results given in figure 6 indicate that, for the basic configura- tion with undeflected ailavator, the zero-lift drag rise began at a Mach number of about 0.85. The drag coefficient increased from a value of 0.012 at speeds below the drag rise to a maximum of about 0.071 at a Mach number of 1.075, a five-fold increase in drag. For the basic configura- tion with the ailavator deflected -8.0°, the zero-lift drag rise began at about the same Mach number, but the increase in drag through the transonic range was slightly less than for the undeflected-ailavator configuration. The results for the speed brakes installed showed that the drag rise occurred at about 0.1 Mach number earlier and also indicated a slightly higher drag rise through the transonic range than for the basic configu- ration with undeflected ailavator.

The results presented in figure 11 indicate that the incremental drag produced by -8.0° deflection of the ailavator, in general, increased with increase in normal-force coefficient at a given Mach number. In general, the values of incremental drag produced by -8.0° deflection of the ailavator were smaller at speeds above than at speeds below the drag rise. The incremental drag coefficients produced by installation of the speed brakes showed no consistent changes with changes in normal-force coefficient and Mach number but had values of from 0.040 to 0.074 depending on the values of normal-force coefficient and Mach number. These values correspond to drag coefficients of about 0.40 and 0.75 based

on speed-brake frontal area. The incremental drag between the fin-off
and fin-on configurations varied from negative values at speeds below
the drag rise to positive values during the drag rise, and then to nega-
tive values at supersonic speeds. The value of incremental drag varied
from 0.009 to -0.009 depending on the normal-force coefficient and Mach
number. The positive values of incremental drag between the fin-off and
fin-on configurations at speeds during the drag rise may be the result of
a favorable effect of the fin on the flow over the outer wing panel. A
positive increment in drag coefficient between the fin-off and fin-on
configurations was also indicated in the tests of reference 3 at Mach
numbers between about 0.94 and 0.97. It should also be noted that over
the Mach number region covering the drag rise, the incremental drag
results presented are subject to some inaccuracy which arises from the
error of measurement of Mach number, together with the steepness of the
curves of drag coefficient against Mach number in this region.

Normal-Force Results

The results given in figure 14 indicate that at Mach numbers up to
about 0.85, the normal-force-curve slope of the fin-off configuration is
somewhat higher at low ailavator deflections than the slope of the fin-
on configuration. At Mach numbers above about 0.90, the normal-force-
curve slope of the fin-off configuration is appreciably lower at all
ailavator deflections than the slope of the fin-on configuration. Exami-
nation of the results shown in figure 15 indicates that there are no
consistent differences in the normal-force-curve slope with speed brakes
on and off except in the region near $M = 1.0$ where the slope with the
speed brakes on is somewhat higher.

Longitudinal-Stability Results

The results given in figure 18 indicate that removal of the fin, in
general, causes a small forward shift in the neutral point location at
Mach numbers up to about 0.90 for all ailavator deflections tested. At
Mach numbers above about 0.90, removal of the fin causes a considerable
forward movement of the neutral-point location. With the fin removed,
with increase in Mach number from about 0.91 to 0.96, a large forward
shift in the neutral-point location occurs for the undeflected-ailavator
configuration with the result that a negative value of the static margin
(c.g. at 17 percent M.A.C.) is reached at Mach numbers between about 0.94
and 0.975. It should be noted that the ailavator deflection required for
trim at these speeds, however, would be a rather large negative value
because of loss of ailavator effectiveness in this region and that, for
ailavator deflections of -4.9° and -8.0°, the forward shift in the neutral-
point location is small and the static margin always remains positive.
The results of reference 4 for the undeflected-ailavator configuration

indicated, in general, only a slight forward shift in the neutral-point
location on removal of the fin for Mach numbers up to 0.90. Beyond a
Mach number of 0.90, a tendency toward a forward shift is evident. The
addition of the speed brakes, figure 19, resulted in a considerable
forward shift in the neutral-point location throughout the Mach number
range. The results of the tests of reference 4 also indicated a forward
shift in the neutral-point location on addition of the speed brakes but
the shift was of smaller magnitude than that of the present tests. The
static margin was reduced by addition of the speed brakes to a value of
2 or 3 percent mean aerodynamic chord depending on the ailavator deflec-
tion, at Mach numbers in the region of 0.80 to 0.85.

Longitudinal-Control Effectiveness Results

The results shown in figure 20 indicate that, with the fin off,
ailavator ineffectiveness or reversal at low deflections occurs over
approximately the same Mach number range (0.93 to 1.0) as was found for
the fin-on results (reference 1). It appears, however, that with the
fin off a larger reversal of ailavator effectiveness occurs than with
the fin on in this Mach number range. In general, at Mach numbers both
above and below the region from 0.93 to 1.0, the ailavator effectiveness
with fin off over the deflection range tested was less than the effec-
tiveness with the fin on. The results given in figure 21 indicate that
for 0° to -8.0° deflection of the ailavator, with the speed brakes on,
there is little or no reduction in ailavator effectiveness in the Mach
number range from 0.85 to 1.0 as is evident for the configuration with
speed brakes off. The results taken from reference 4 for speed brakes
on and off at ailavator deflections of 0° and -4.4° also appear to
indicate, in general, less reduction in ailavator effectiveness with
speed brakes on than with speed brakes off at Mach numbers from about
0.85 to 0.91. In general, at Mach numbers below and above the range
from 0.85 to 1.0, the ailavator effectiveness for 0° to -8.0° ailavator
deflection with speed brakes on appears to be of the same magnitude as
that with speed brakes off. From an inspection of figure 22, it is
evident that ailavator ineffectiveness or reversal exists in the Mach
number range from 0.93 to 1.0 for the skewed-hinge-line ailavator similar
to that which exists for the original ailavators.

CONCLUDING REMARKS

The results of NACA wing-flow tests of drag, normal-force, pitching-
moment, lift, and angle-of-attack measurements of various configurations
of a semispan model of the XF7U-1 airplane throughout the Mach number
range from 0.65 to 1.10 indicated the following:

The drag increment produced by -8.0° deflection of the ailavator increased with increase in normal-force coefficient and was smaller at speeds above than at speeds below the drag rise. The drag increment produced by installation of the speed brakes varied from 0.040 to 0.074, depending on the normal-force coefficient and Mach number. These values correspond to drag coefficients of about 0.40 to 0.75 based on speed-brake frontal area. Removal of the fin produced a small positive drag increment at a given normal-force coefficient at speeds during the drag rise. A large forward shift of the neutral-point location occurred at Mach numbers above about 0.90 upon removal of the fin, and also a considerable forward shift throughout the Mach number range occurred upon installation of the speed brakes. Ailavator ineffectiveness or reversal at low deflections similar to that determined in previous tests of the basic configuration of the model in the Mach number range from about 0.93 to 1.0 was found for the fin-off configuration and for the model equipped with skewed (more highly sweptback) hinge-line ailavators. With the speed brakes installed, little or no loss in the incremental pitching moment produced by deflection of the ailavator from 0° to -8.0° occurred in the Mach number range from 0.85 to 1.0 in contrast to a considerable loss found in previous tests of the basic configuration.

Langley Aeronautical Laboratory
    National Advisory Committee for Aeronautics
        Langley Air Force Base, Va.

Richard H. Sawyer
Aeronautical Research Scientist

James P. Trant, Jr.
Aeronautical Research Scientist

Approved:

Melvin N. Gough
Chief of Flight Research Division

DLMcC

REFERENCES

1. Sawyer, Richard H., and Trant, James P., Jr.: Longitudinal Stability
     and Control Characteristics of a Semispan Model of the XF7U-1 Tail-
     less Airplane at Transonic Speeds by the NACA Wing-Flow Method -
     TED No. NACA DE307. NACA RM L7I08, Bur. Aero., 1947.

2. Johnson, Harold I.: Measurements of Aerodynamic Characteristics of
     a 35° Sweptback NACA 65-009 Airfoil Model with $\frac{1}{4}$-Chord Plain Flap
     by the NACA Wing-Flow Method. NACA RM L7F13, 1947.

3. Goodson, Kenneth W., and King, Thomas J., Jr.: Longitudinal Stability
     and Control Characteristics of a Semispan Wind-Tunnel Model of a
     Tailless Airplane and a Comparison with Complete-Model Wind-Tunnel
     Tests and Semispan-Model Wing-Flow Tests. NACA RM L9C31, 1949.

4. Kuhn, Richard E., and Myers, Boyd C., II: An Investigation of the
     Aerodynamic Characteristics of an 0.08-Scale Model of the Chance
     Vought XF7U-1 Airplane in the Langley High-Speed 7- by 10-Foot
     Tunnel. Part V - Wing-Alone Tests and Effect of Modifications to
     the Vertical Fins, Speed Brakes, and Fuselage - TED No. NACA DE308.
     NACA RM L7J09, Bur. Aero., 1947.

TABLE I

GEOMETRIC CHARACTERISTICS OF MODEL AND OF FULL-SCALE AIRPLANE

Characteristics	Model	Full-scale airplane
Wing:		
Section (perpendicular to 25-percent-chord line)	CVA4-(00)-(12)(40)-(1.1)(1.0)	CVA4-(00)-(12)(40)-(1.1)(1.0)
Semispan	6.03 in.	19 ft 4 in.
M.A.C.	4.08 in.	13 ft 1 in.
Chord at tip	3.02 in.	9 ft 8 in.
Chord at plane of symmetry	4.99 in.	16 ft 0 in.
Area (semispan)	24.2 sq in.	248 sq ft
Taper ratio	0.605	0.605
Aspect ratio	3.01	3.01
Sweepback (25-percent-chord line) . . .	35°	35°
Incidence (constant)	0°	0°
Dihedral	0°	0°
Ailavator:		
Semispan	2.94 in.	9 ft 5 in.
Chord (parallel to plane of symmetry)	0.91 in.	35 in.
Area (one)	2.68 sq in.	27.5 sq ft
Sweepback	24.5°	24.5°
Vertical tail:		
Area of one (including wing intersection area)	6.24 sq in.	64 sq ft
Aspect ratio	1.75	1.75
Sweepback (25-percent-chord line) . . .	40°	40°
Speed brakes:		
Area:		
Upper (one)	1.24 sq in.	12.7 sq ft
Lower (one)	1.15 sq in.	11.8 sq ft
Deflection from chord line:		
Upper	35°	35°
Lower	35°	35°
Fuselage:		
Area of maximum cross section (1/2 fuselage)	0.792 sq in.	8.14 sq ft
Area of engine bulge (one)	0.340 sq in.	3.49 sq ft
Over-all length	11.54 in.	37 ft
Air ducts:		
Area of entrance (one)	0.156 sq in.	1.60 sq ft
Area of exit (one)	0.134 sq in.	1.38 sq ft
Location of c.g.	17 percent M.A.C.	17 percent M.A.C.
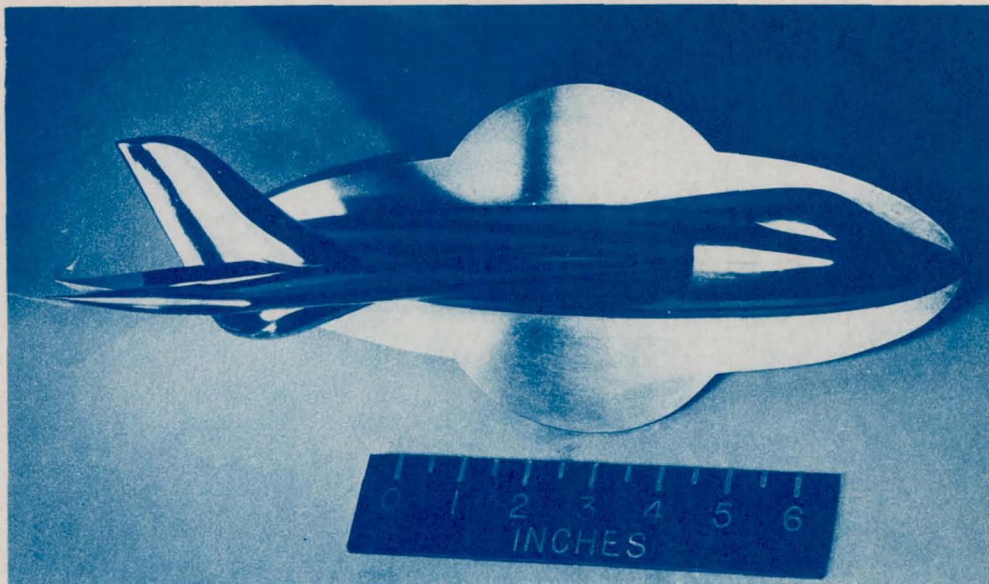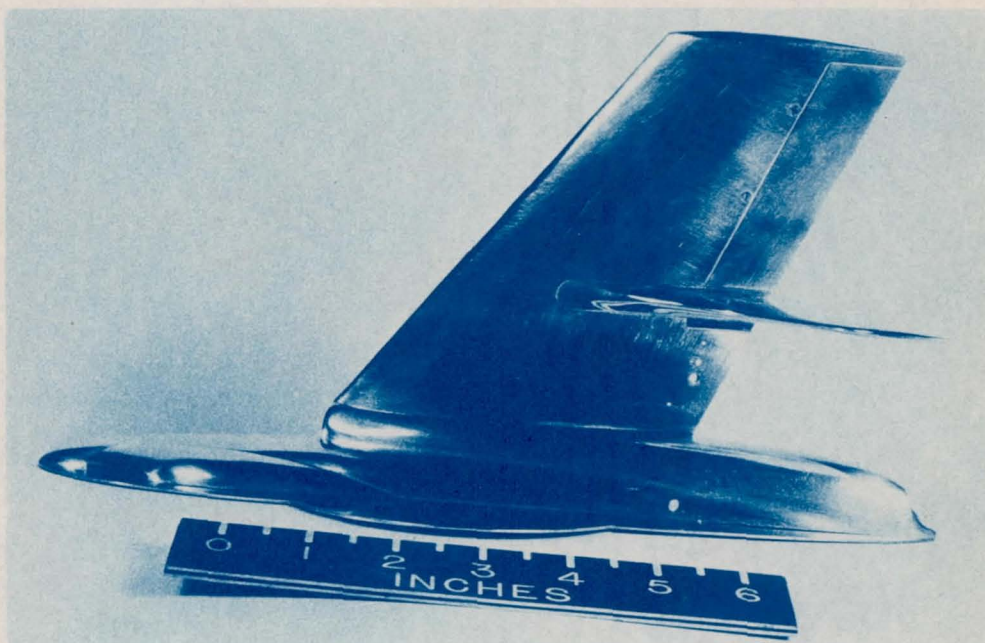
L-50109

L-50106

Figure 1.- XF7U-1 semispan model. Basic configuration.
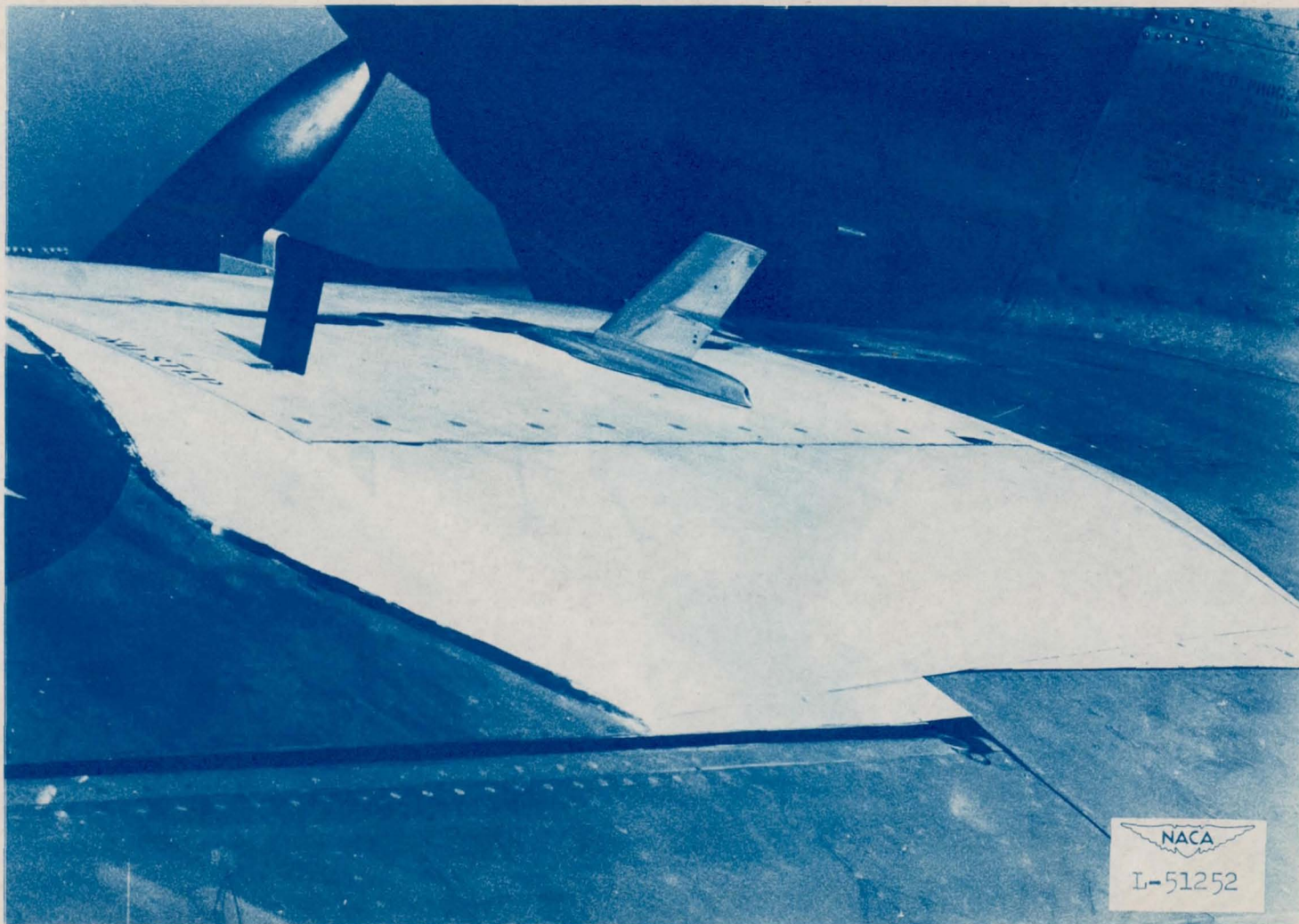
Figure 2.- XF7U-1 semispan model mounted above wing of F-51D airplane. Free-floating vane also shown.

VERTICAL TAIL

4.99 DIAMETER

11.54

FUSELAGE

ENDPLATE

SPEED BRAKE #1

SPEED BRAKE #2

SKEWED HINGE LINE

3.02

35°

25-PERCENT-CHORD LINE

0.91

AILAVATOR

35°

DUCT

2.94

5.77

2.83

2.60

1.07

4.76

SPEED BRAKE

6.72

3°34'

6.03

F-51 D AMMUNITION COMPARTMENT DOOR (MODIFIED)

MOUNTING SHANK

4.99

2.95

No.	A	B	C	θ	φ	X
1	1.690	1.442	.520	29°25'	14°45'	.923
2	1.660	1.442	.470	25°25'	14°45'	.829

SPEED-BRAKE DETAILS
#2 SHOWN #1 SYM. OPP.

NACA
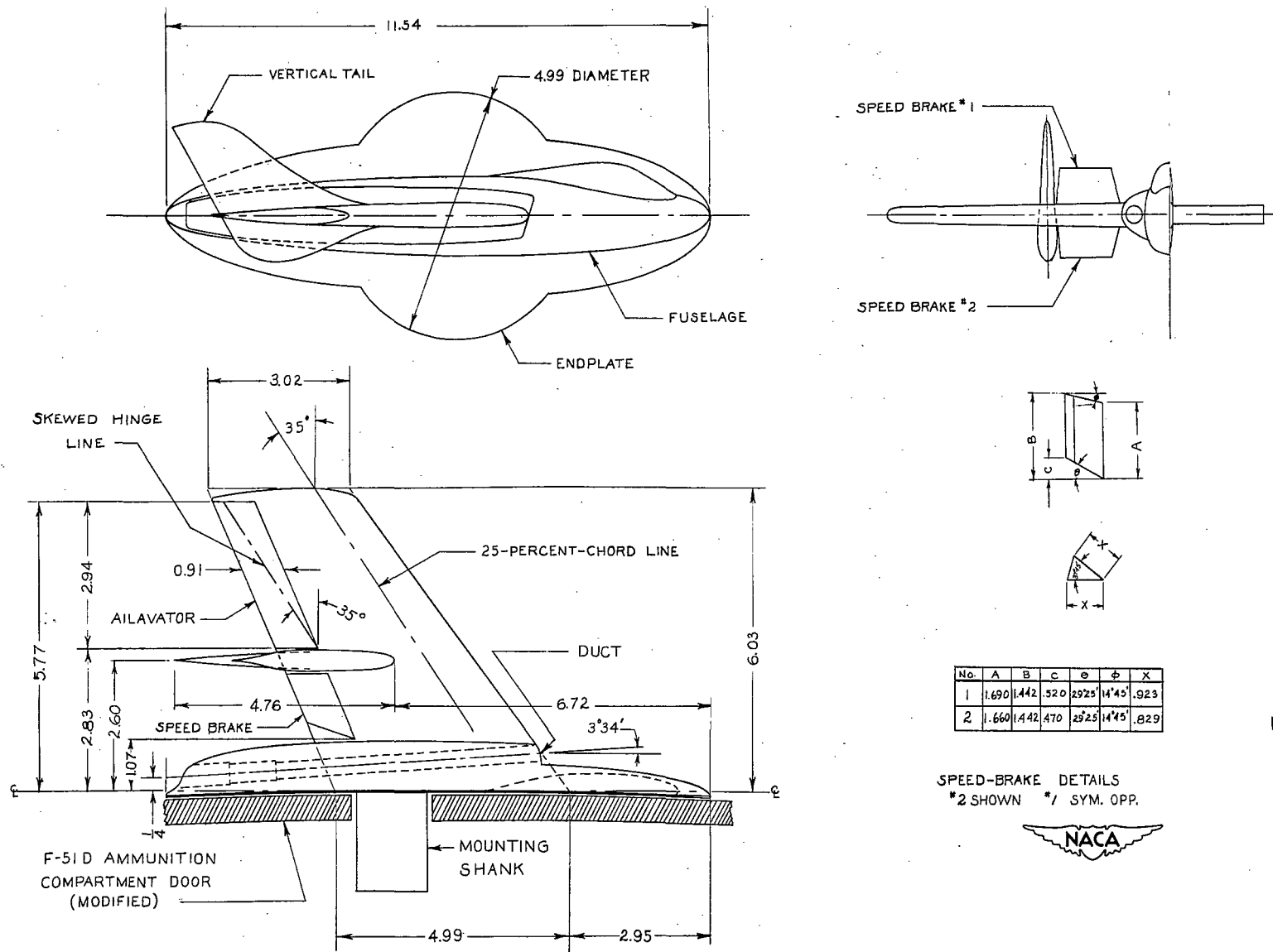
Figure 3.- Details of semispan XF7U-1 model. All dimensions are in inches.
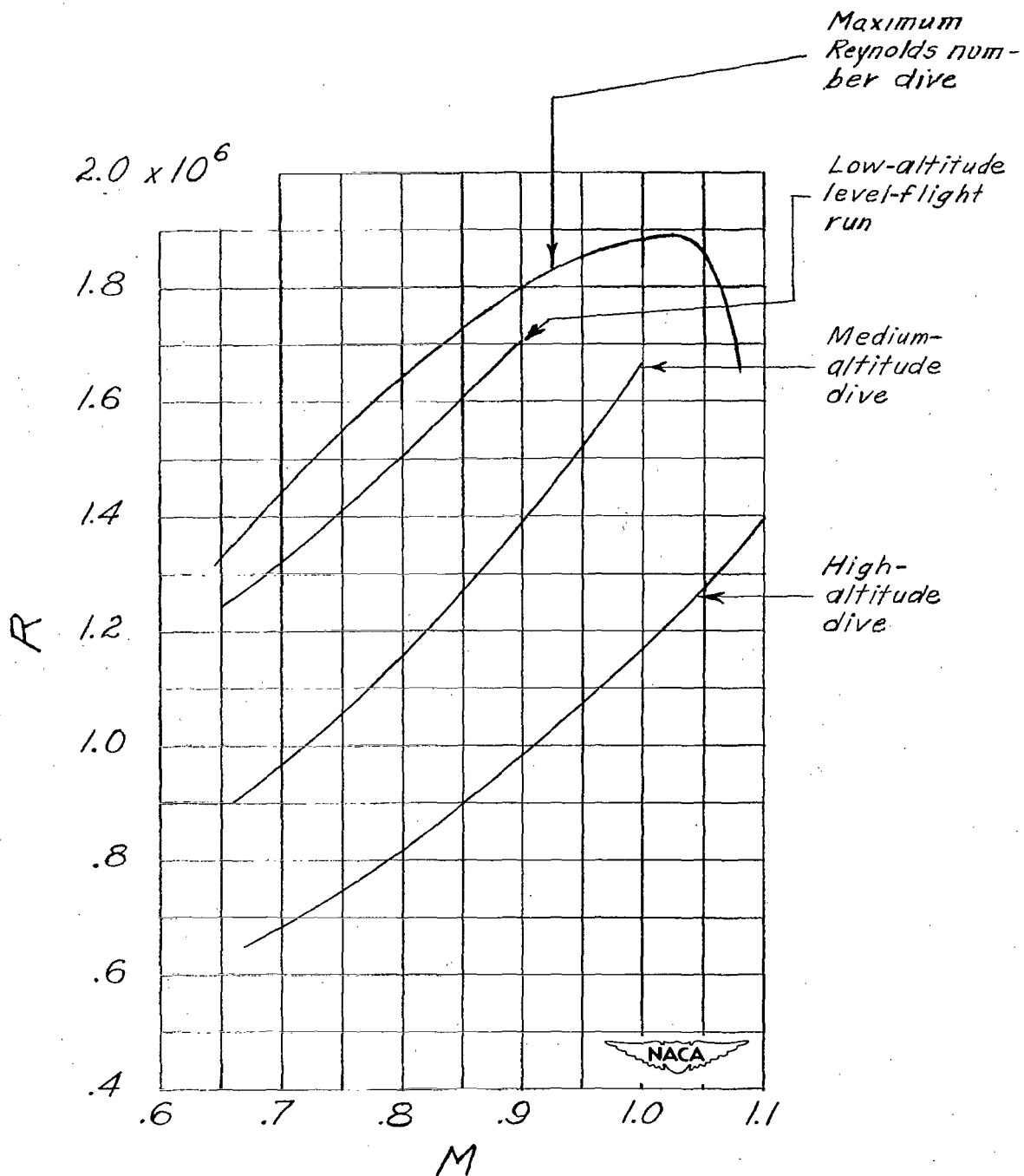
Figure 4.- Variation of Reynolds number with Mach number for tests in high-altitude and medium-altitude dives, in low-altitude, level-flight run, and in maximum Reynolds number dive.
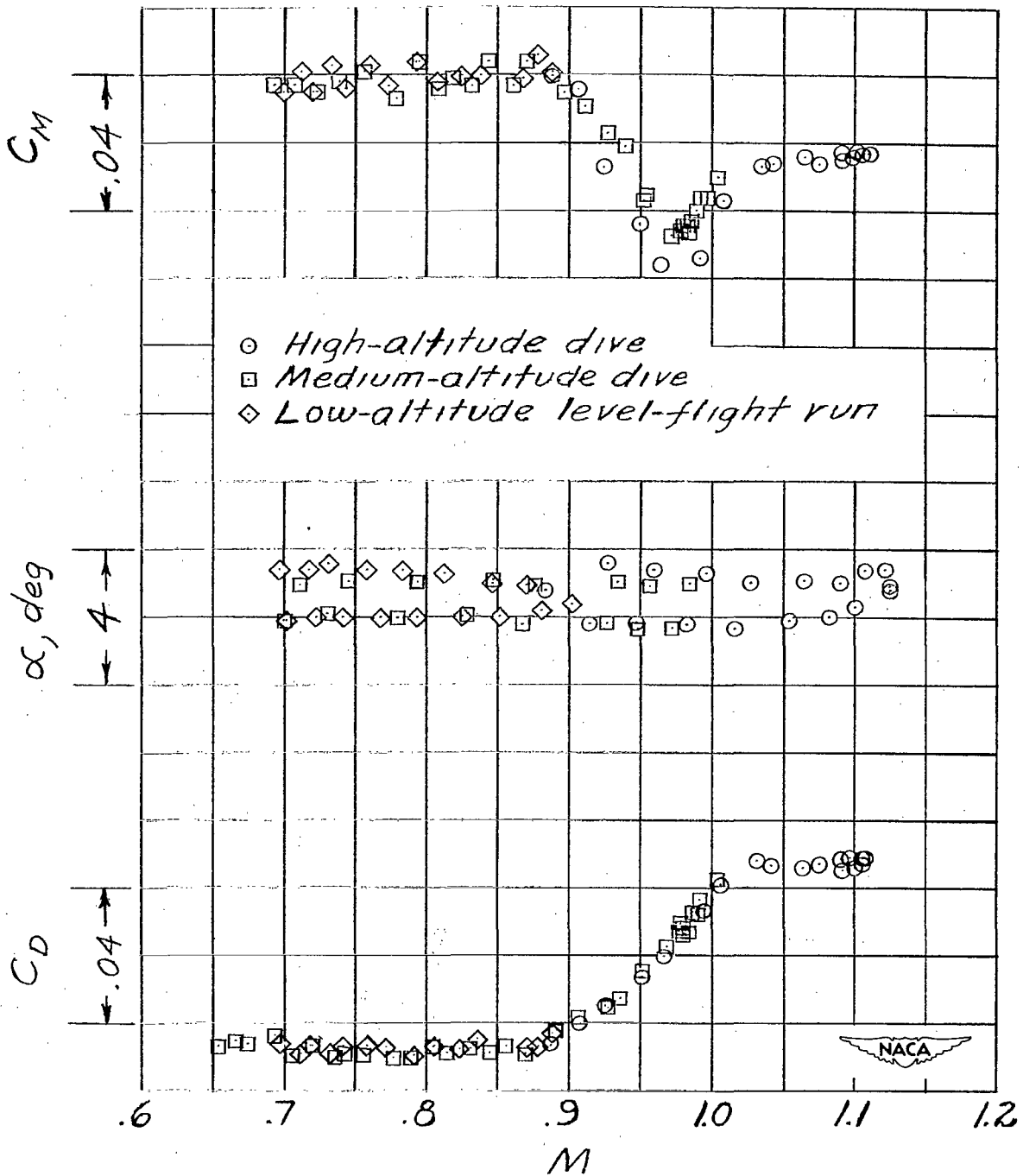
Figure 5.- Typical examples of data as obtained in tests at three altitudes. $C_N = 0$.
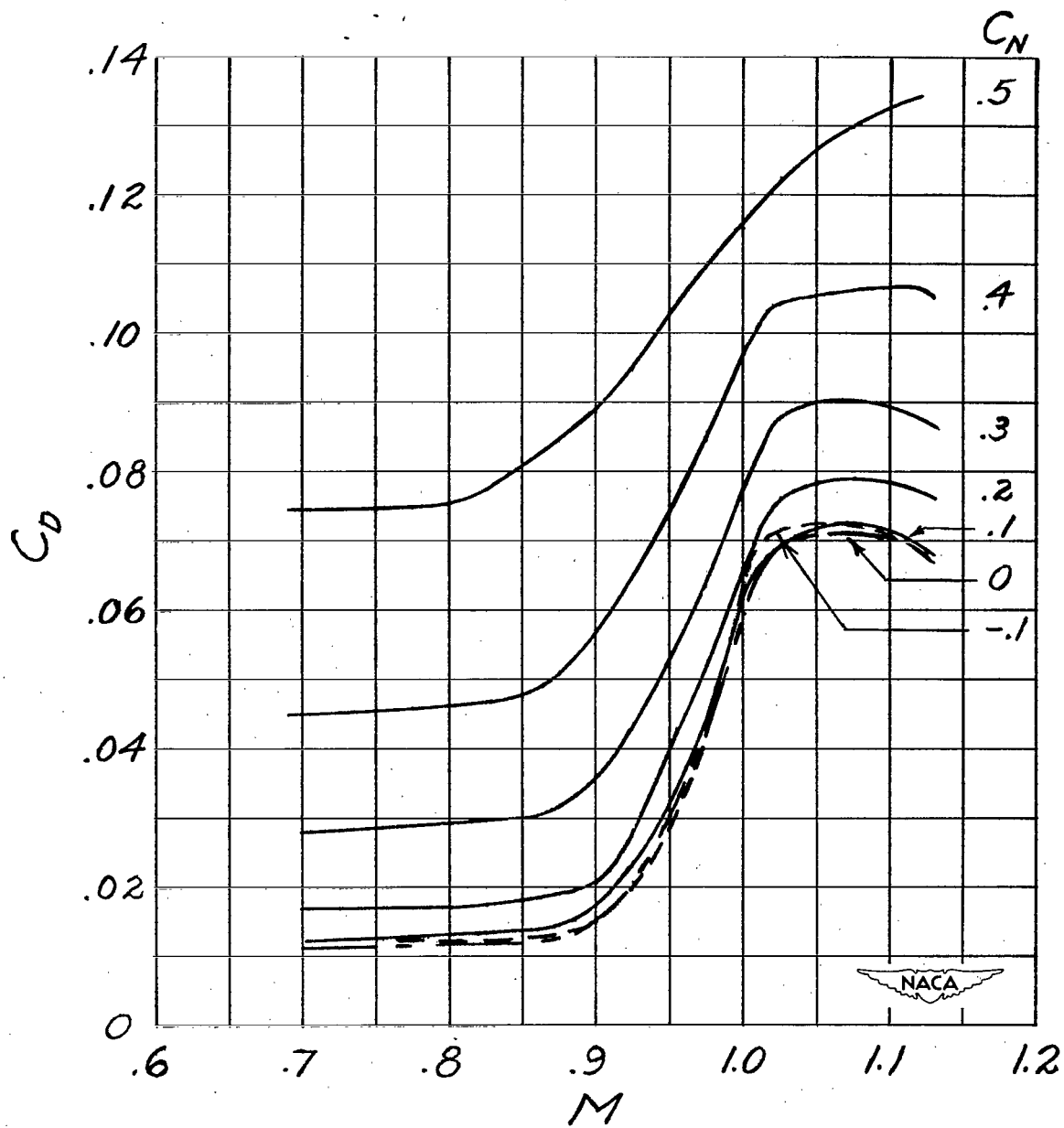
(a) Basic configuration, $\delta_a = 0°$.

Figure 6.- Variation of drag coefficient with Mach number for several values of normal-force coefficient for three model configurations.
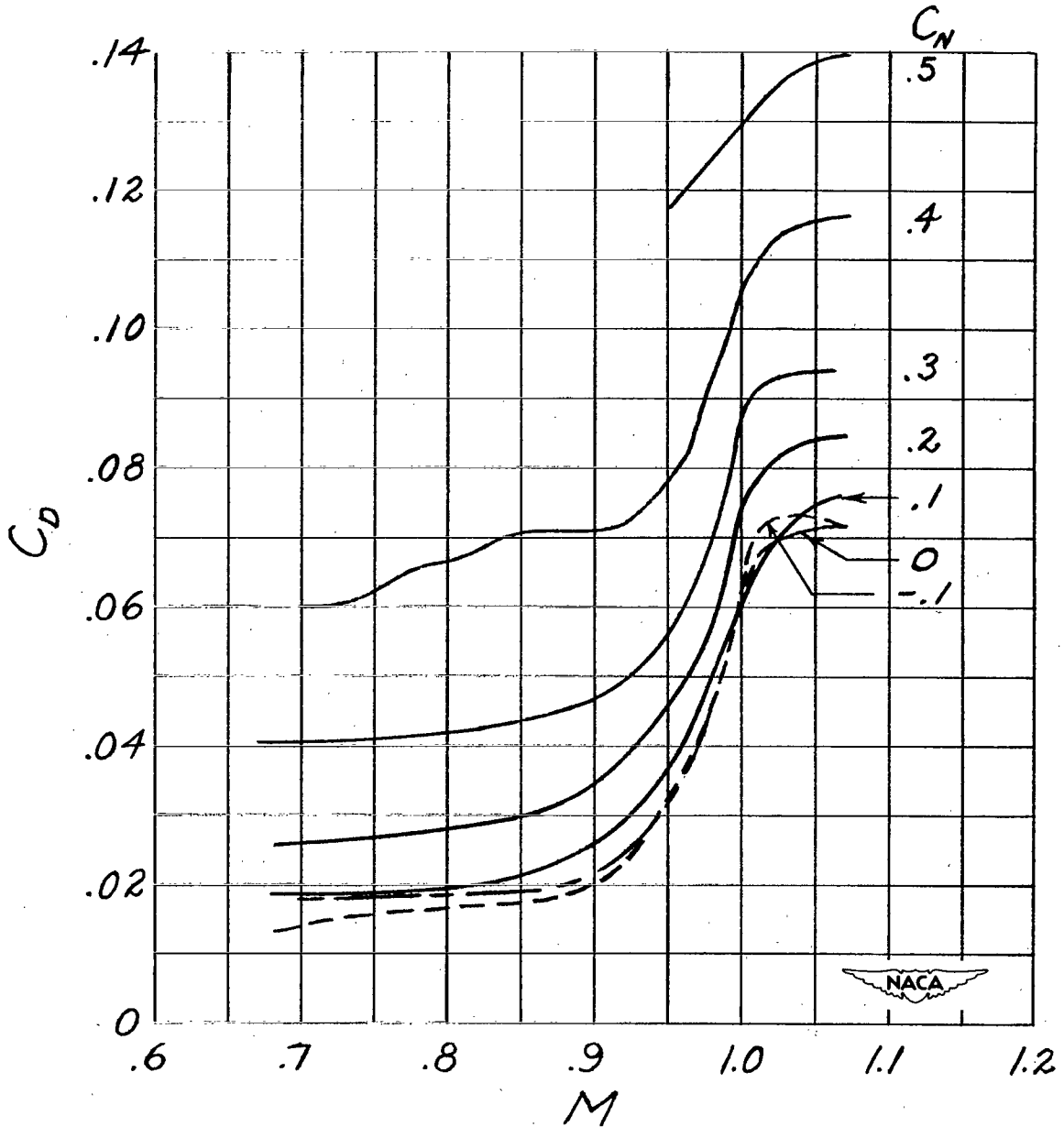
(b) Basic configuration, $\delta_a = -8^\circ$.

Figure 6.- Continued.
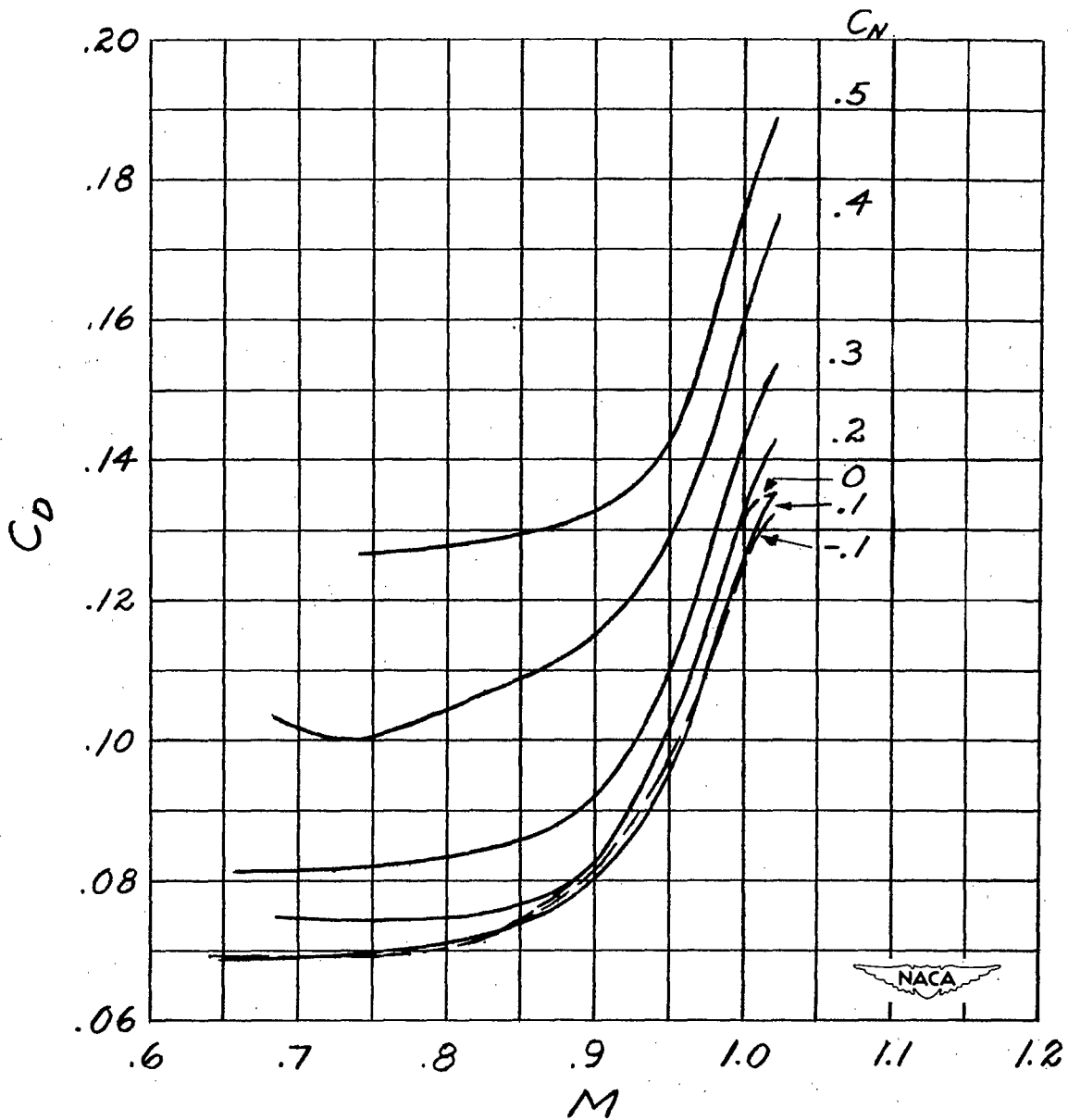
(c) Speed brakes installed. $\delta_a = 0^{\circ}$.

Figure 6.- Concluded.
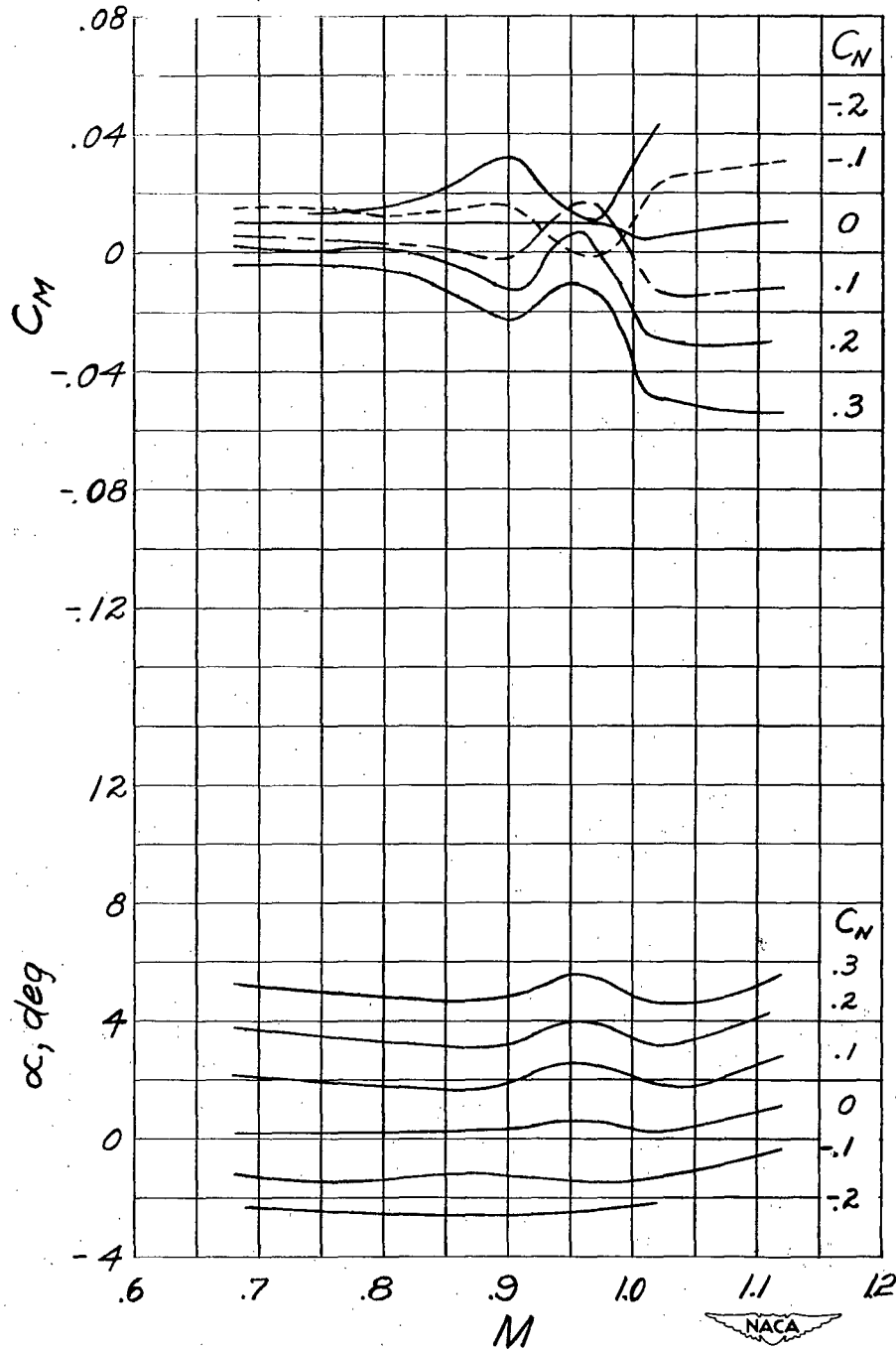
(a) $\delta_a = 0°$.

Figure 7.- Variation of pitching-moment coefficient and angle of attack
with Mach number at several normal-force coefficients for several
ailavator deflections with fin removed.
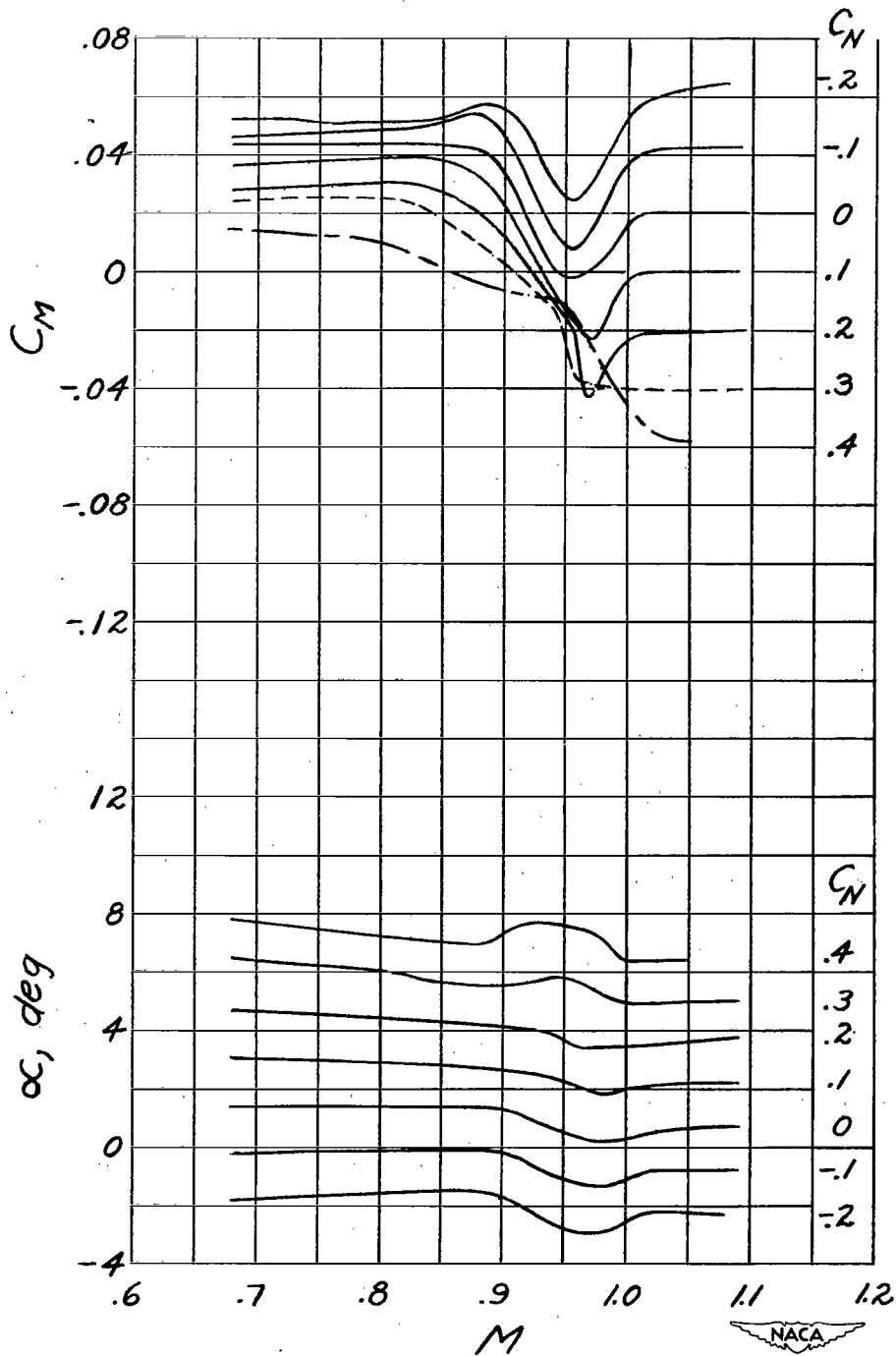
(b) $\delta_a = -4.9°.$

Figure 7.- Continued.
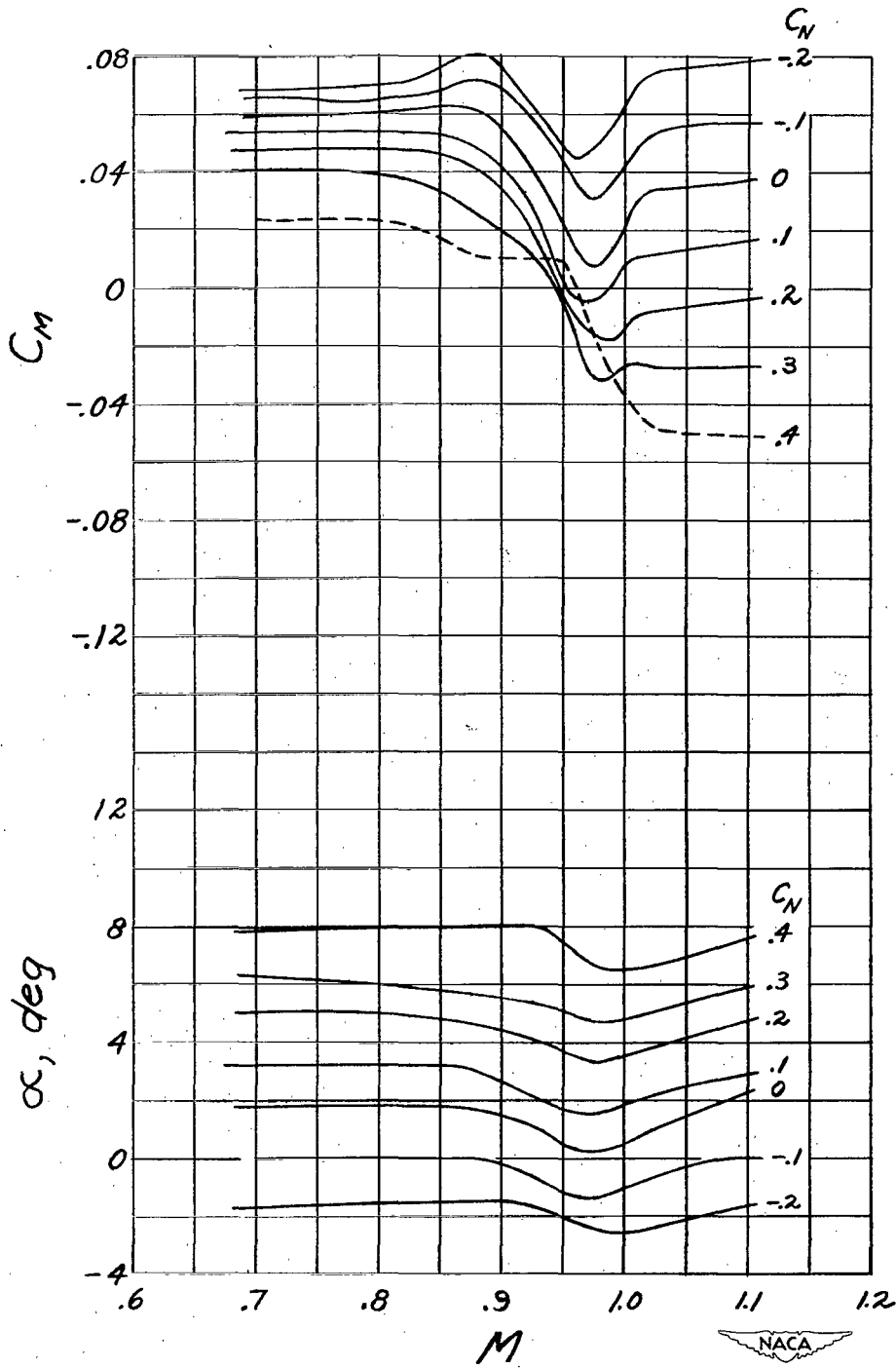
(c) $\delta_a = -8.0°$.

Figure 7.- Concluded.

(a) $\delta_a = 0^o$.
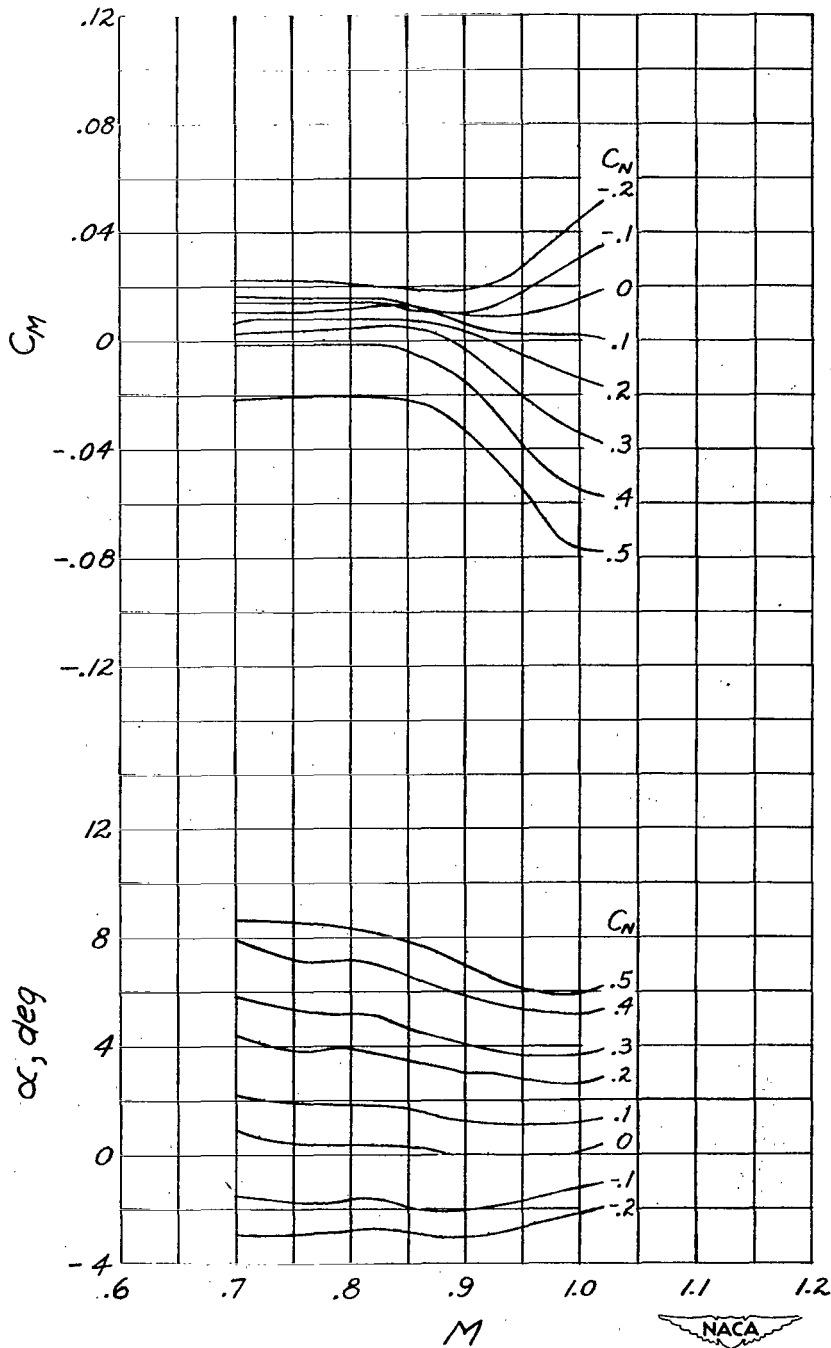
Figure 8.- Variation of pitching-moment coefficient and angle of attack
with Mach number at several normal-force coefficients for two ailavator
deflections with speed brakes installed.
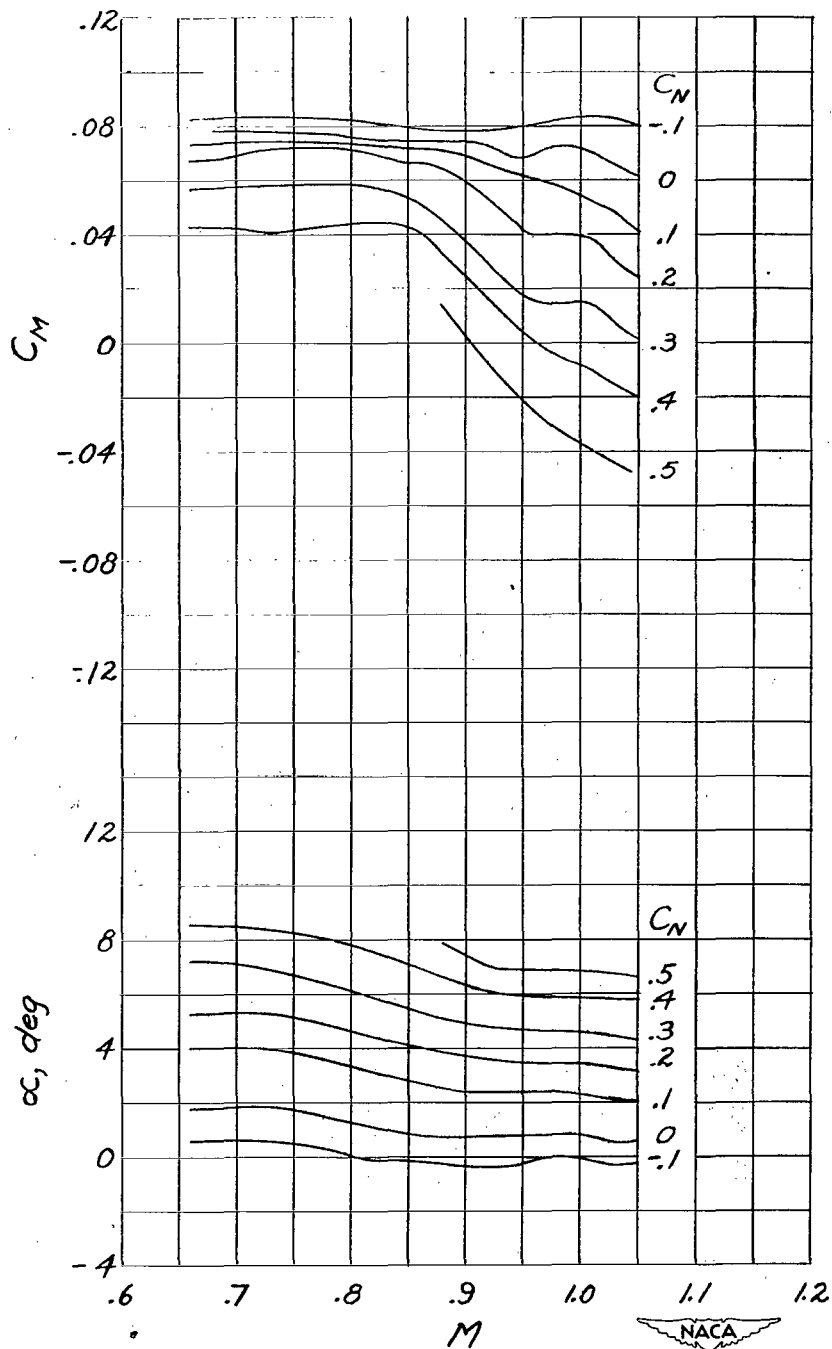
(b) $\delta_a = -8.0°$.

Figure 8.- Concluded.
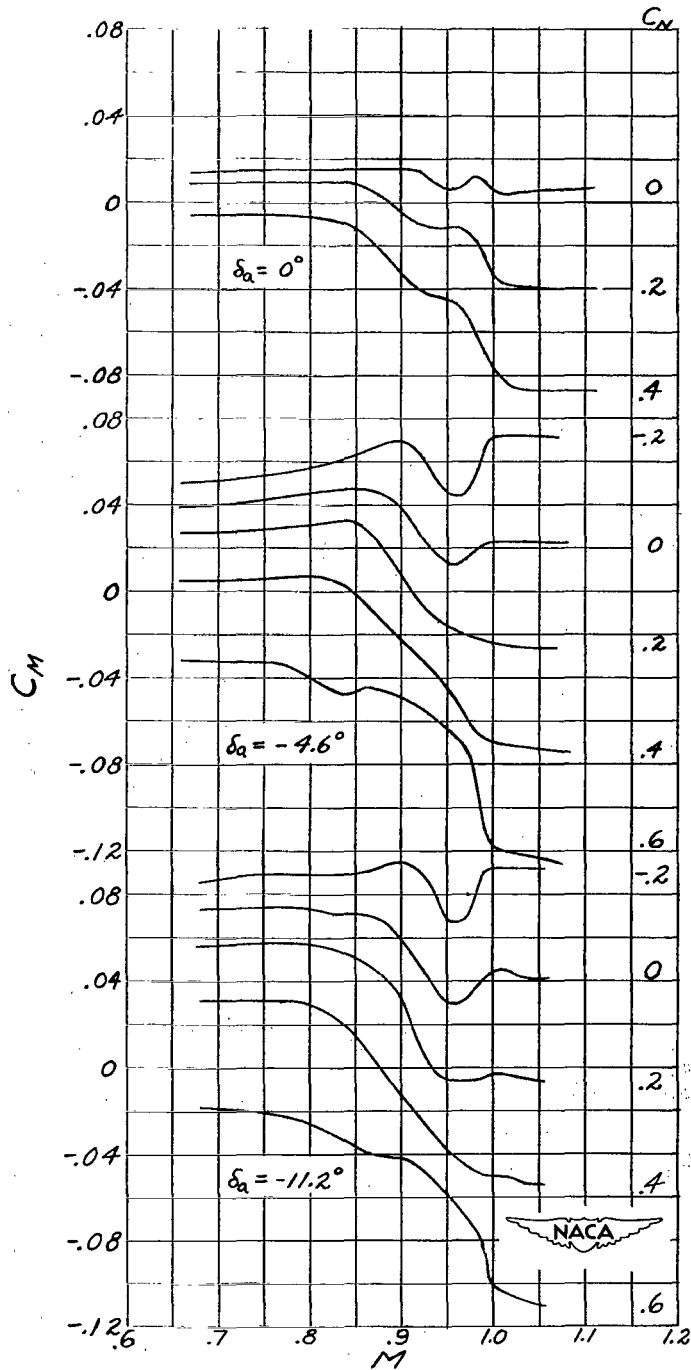
Figure 9.- Variation of pitching-moment coefficient with Mach number
at several normal-force coefficients for several deflections of
ailavators with highly sweptback hinge line.
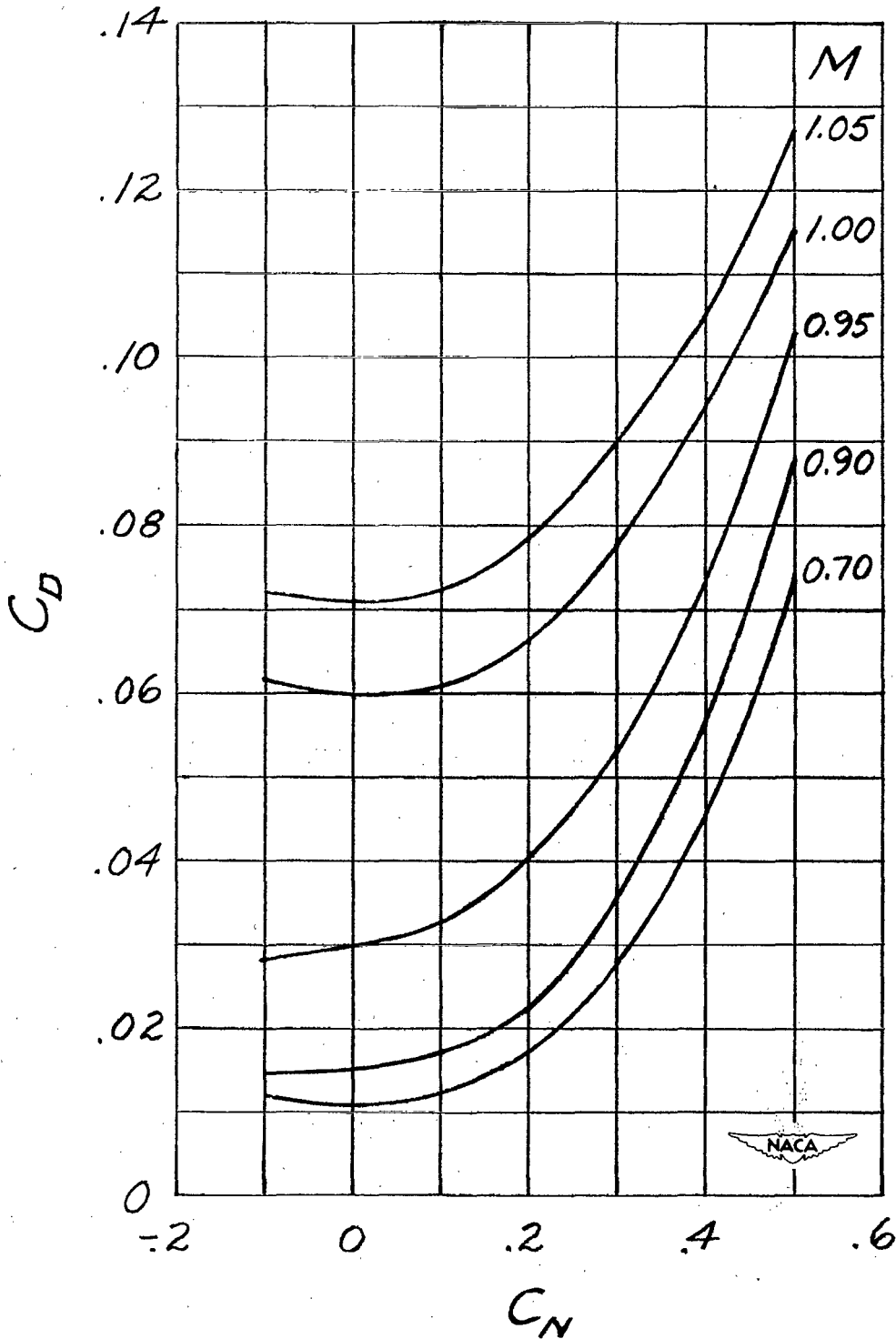
(a) Basic configuration, $\delta_a = 0^\circ$.

Figure 10.- Variation of drag coefficient with normal-force coefficient
at several values of Mach number for three model configurations.
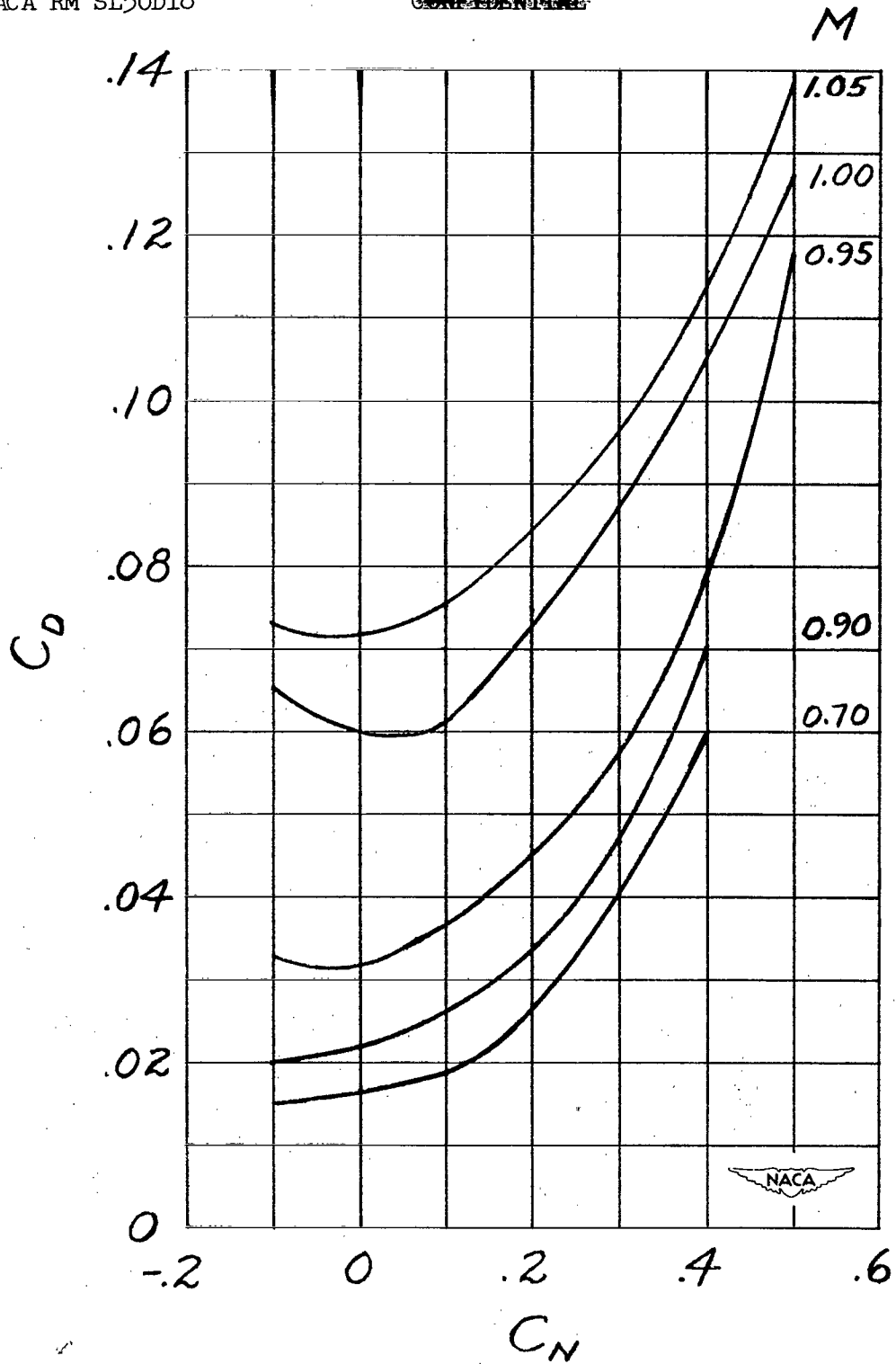
(b) Basic configuration, $\delta_a = -8°$.

Figure 10.- Continued.
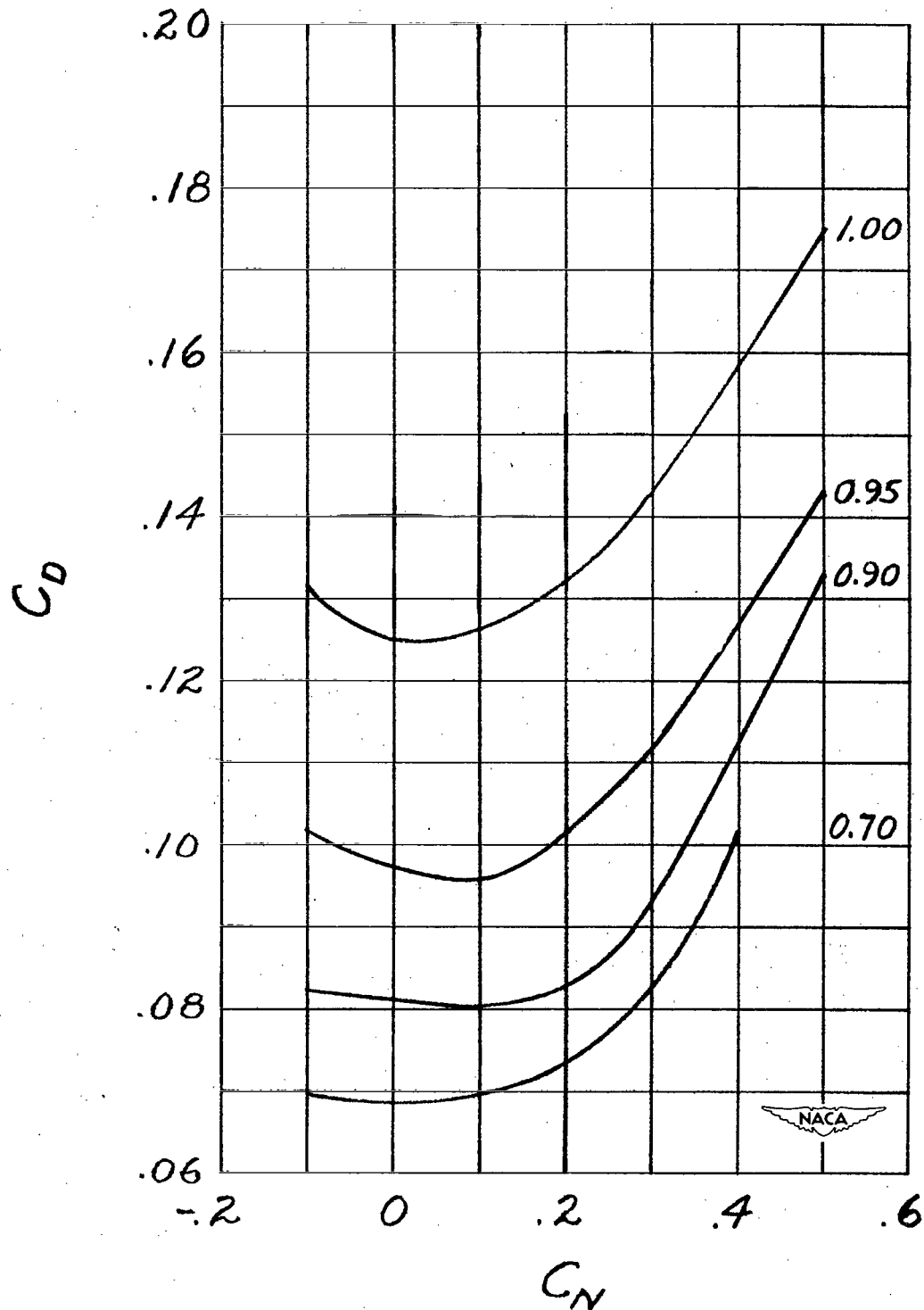
(c) Speed brakes installed, $\delta_a = 0°$.

Figure 10.- Concluded.
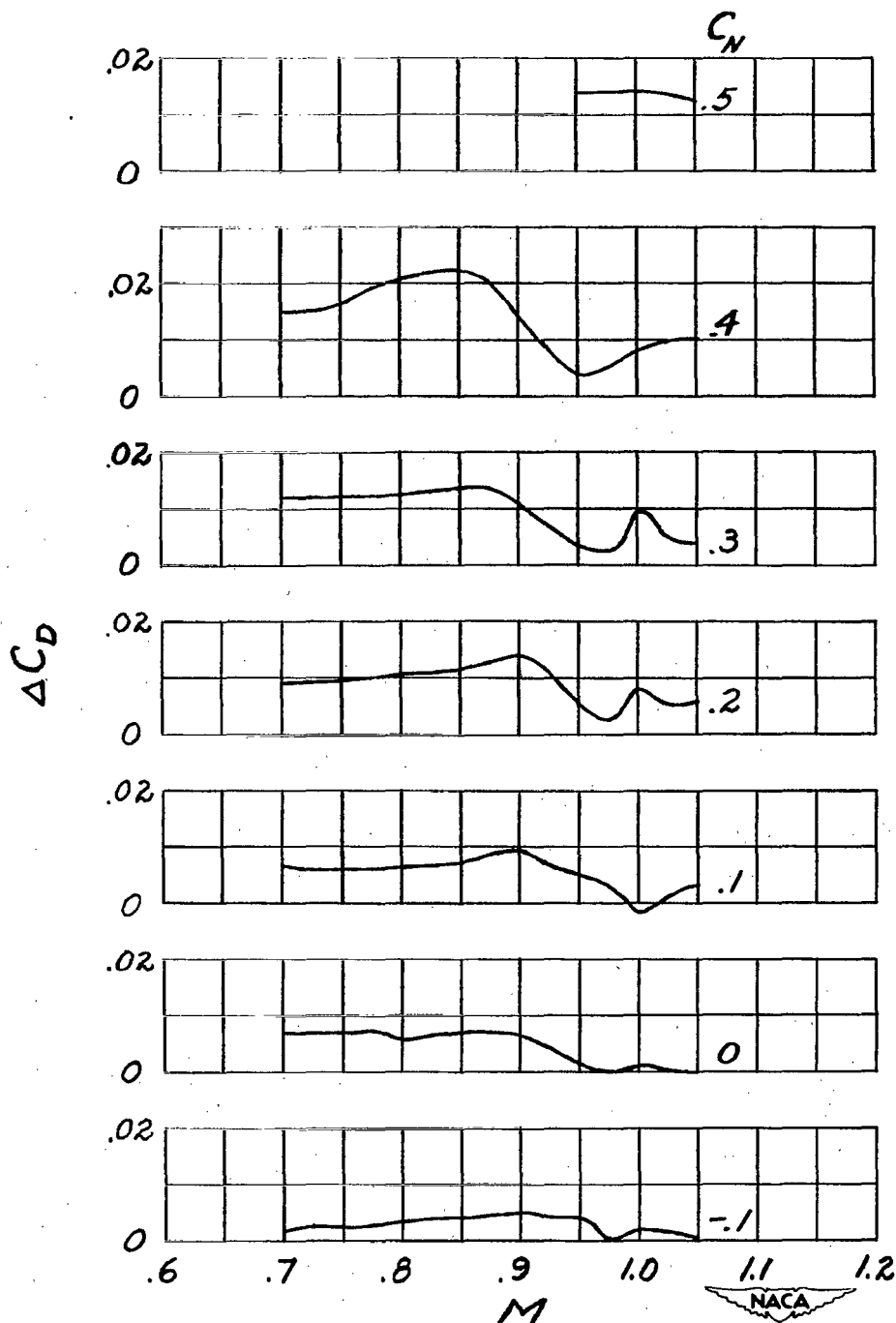
(a) Ailavator deflection of -8°.

Figure 11.- Variation of increment in drag coefficient with Mach number
at several normal-force coefficients for several changes in model
configuration from the basic configuration with undeflected ailavator.
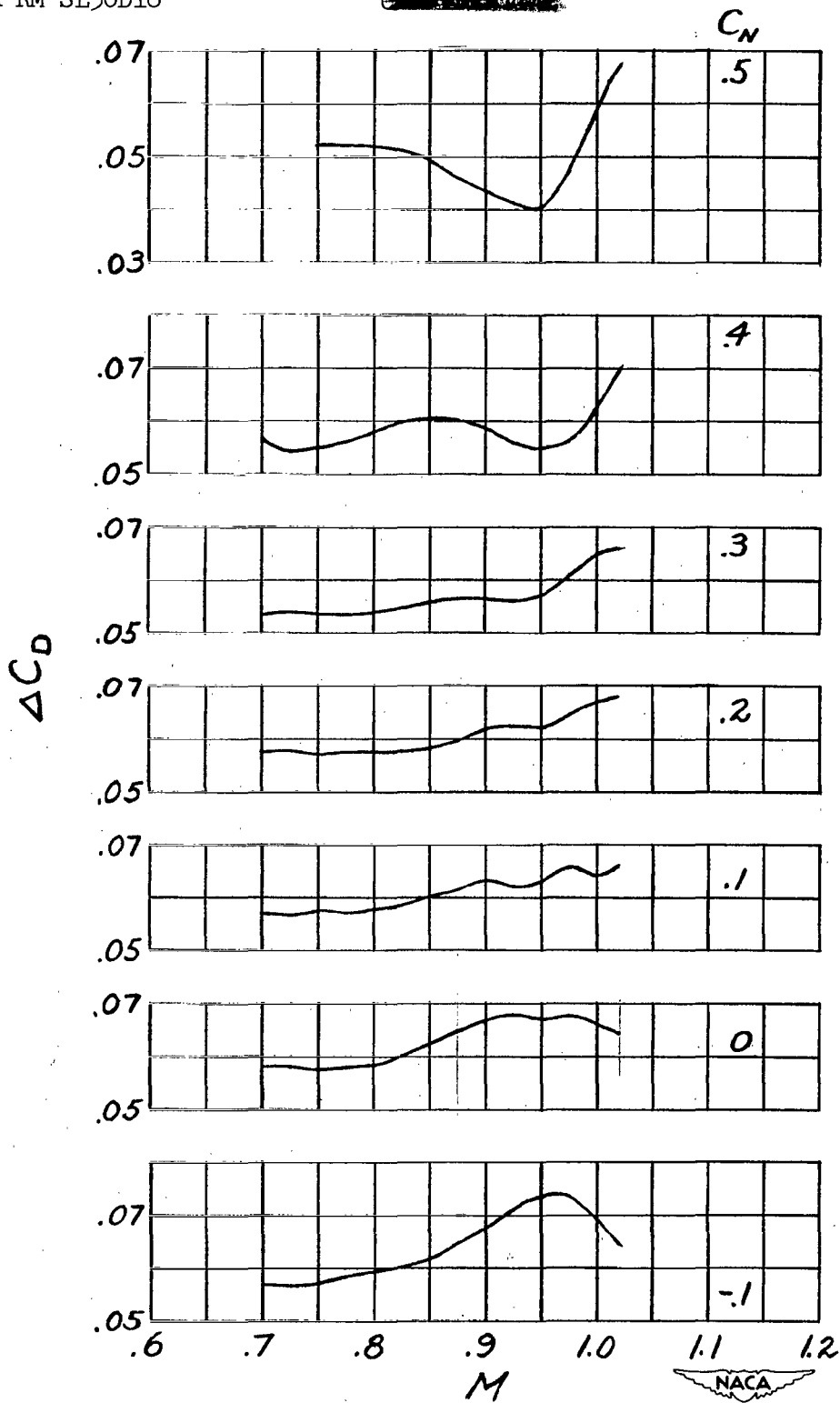
(b) Installation of speed brakes.

Figure 11.- Continued.
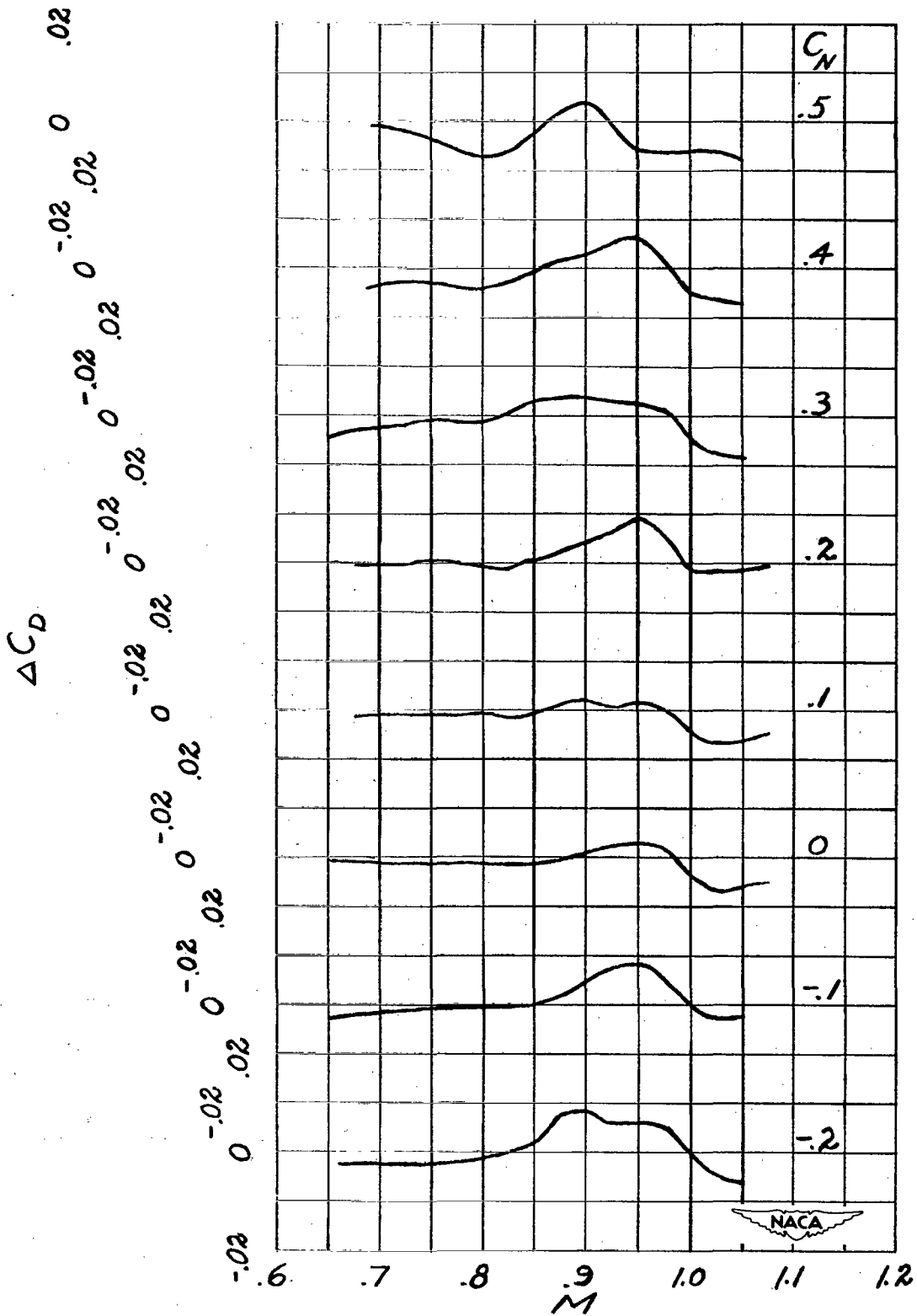
(c) Removal of vertical tail.

Figure 11.- Concluded.
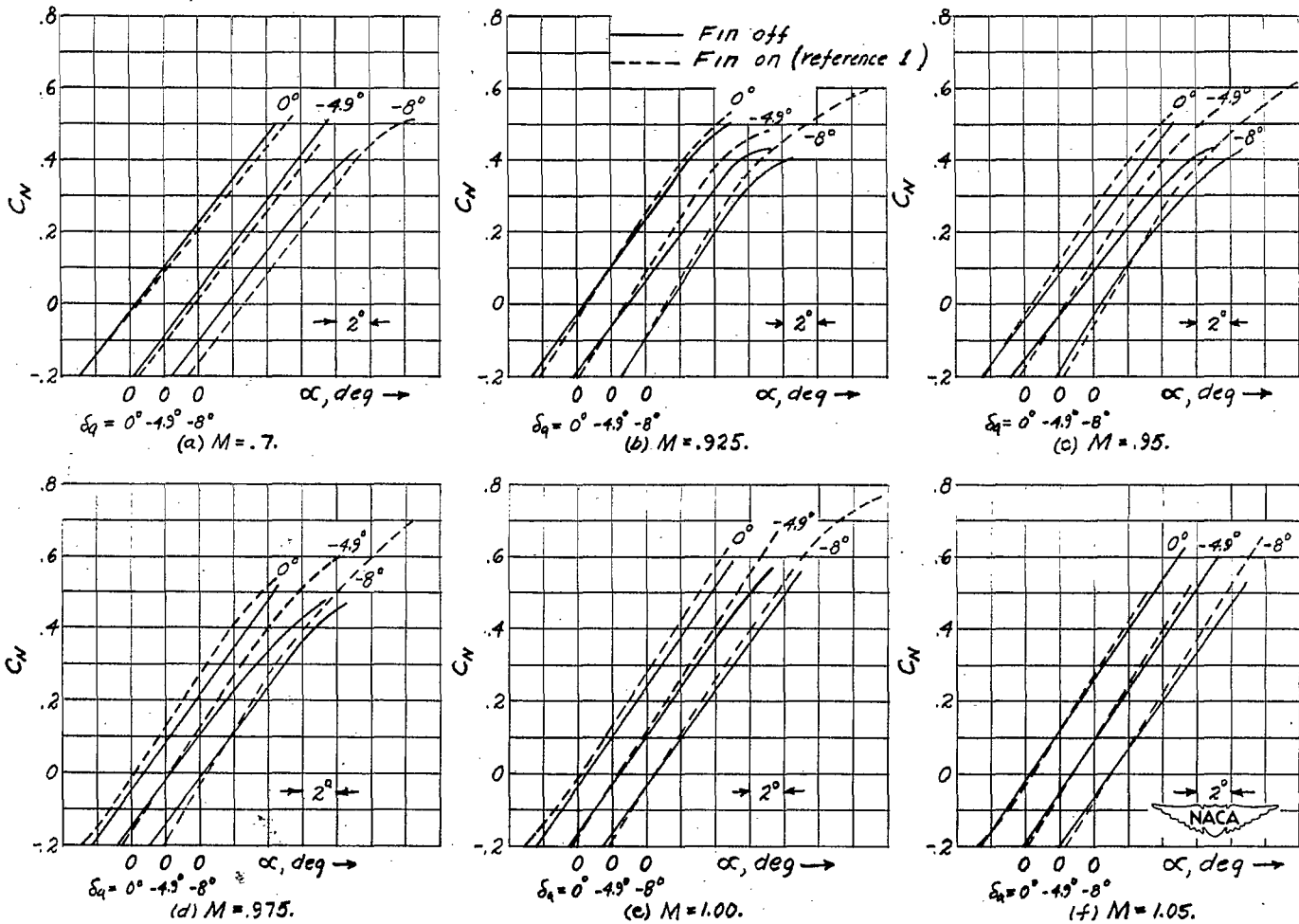
Figure 12.- Variation of normal-force coefficient with angle of attack
at several Mach numbers for several ailavator deflections with fin
removed. Results from reference 1 with fin on shown for comparison.
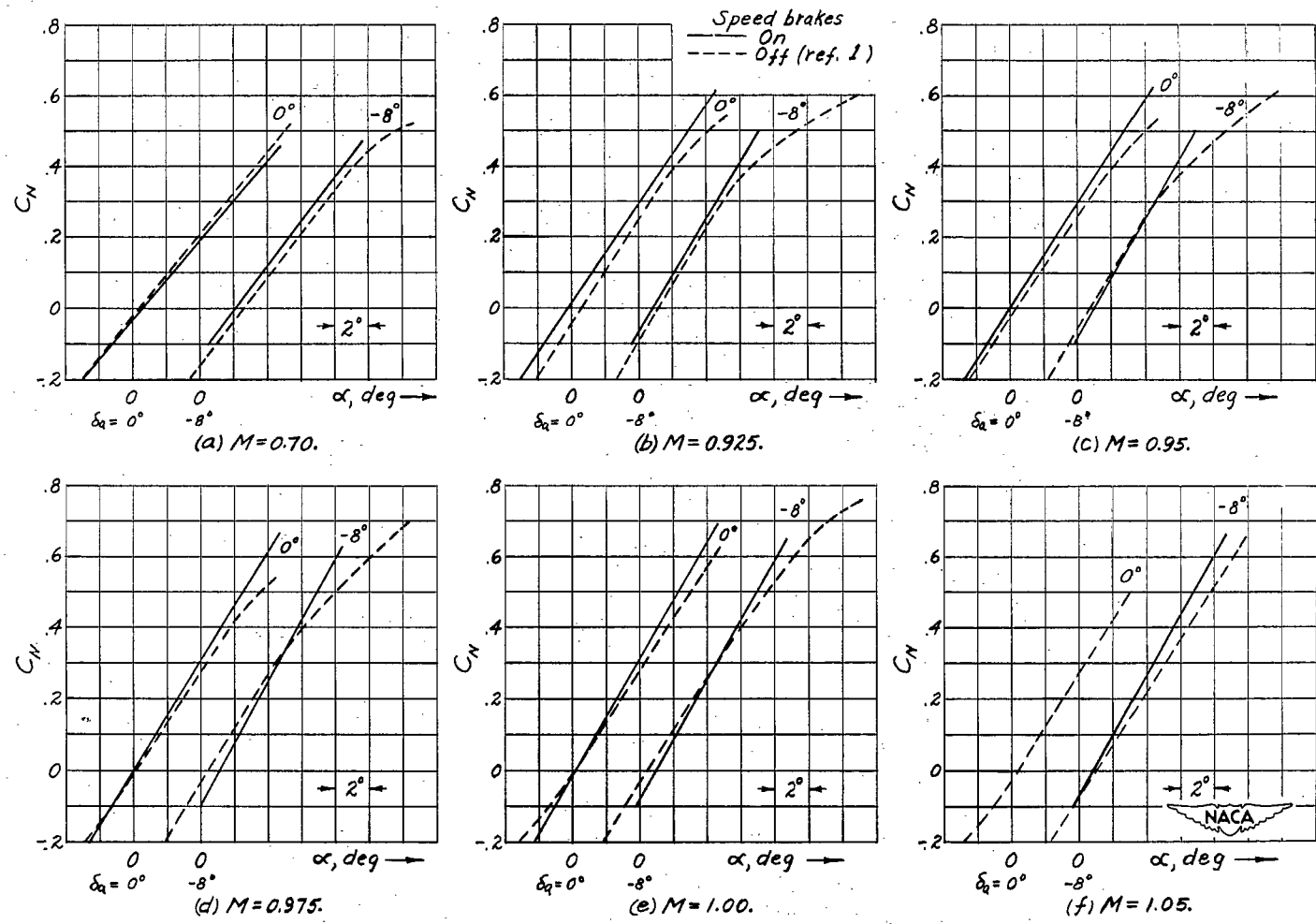
Figure 13.- Variation of normal-force coefficient with angle of attack
at several Mach numbers for two ailavator deflections with speed
brakes on. Results from reference 1 with speed brakes off shown
for comparison.

_____ Fin off

_ _ _ _ _ _ Fin on (reference 1)

$\delta C_N / \delta \alpha$

.08

.04

(a) $\delta_q = 0°$.

.08

.04

(b) $\delta_q = -4.9°$.

.08

.04

.6   .7   .8   .9   1.0   1.1

M
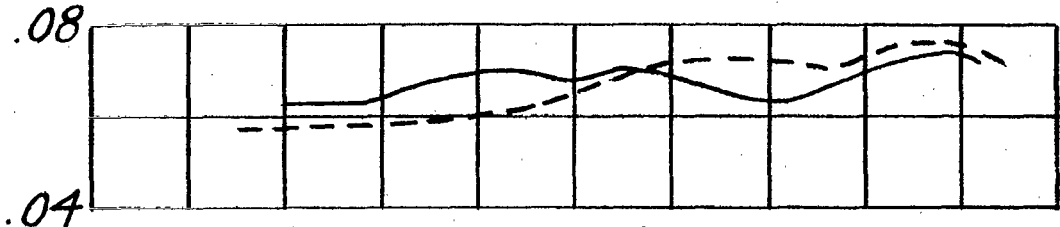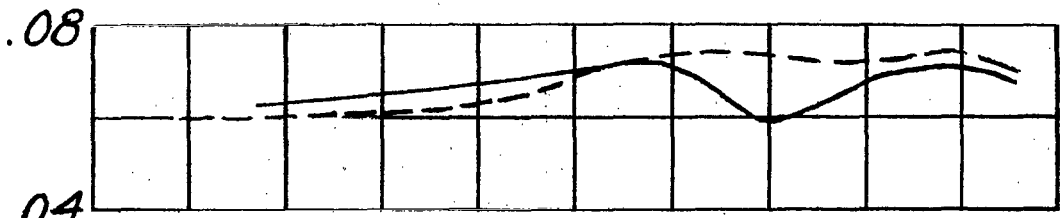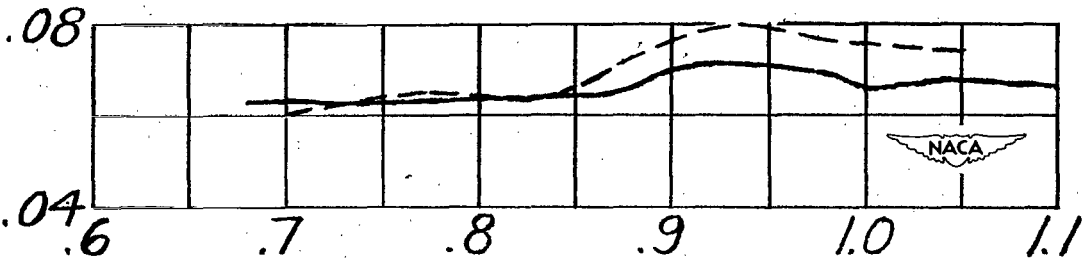
(c) $\delta_q = -8°$.

Figure 14.- Variation of normal-force-curve slope with Mach number for several ailavator deflections with fin off. Results from reference 1 with fin on shown for comparison.

Speed brakes

———— On
————— Off (ref. 1)

$\dfrac{\partial C_N}{\partial \alpha}$

(a) $\delta_Q = 0°$.

(b) $\delta_Q = -8°$.

M
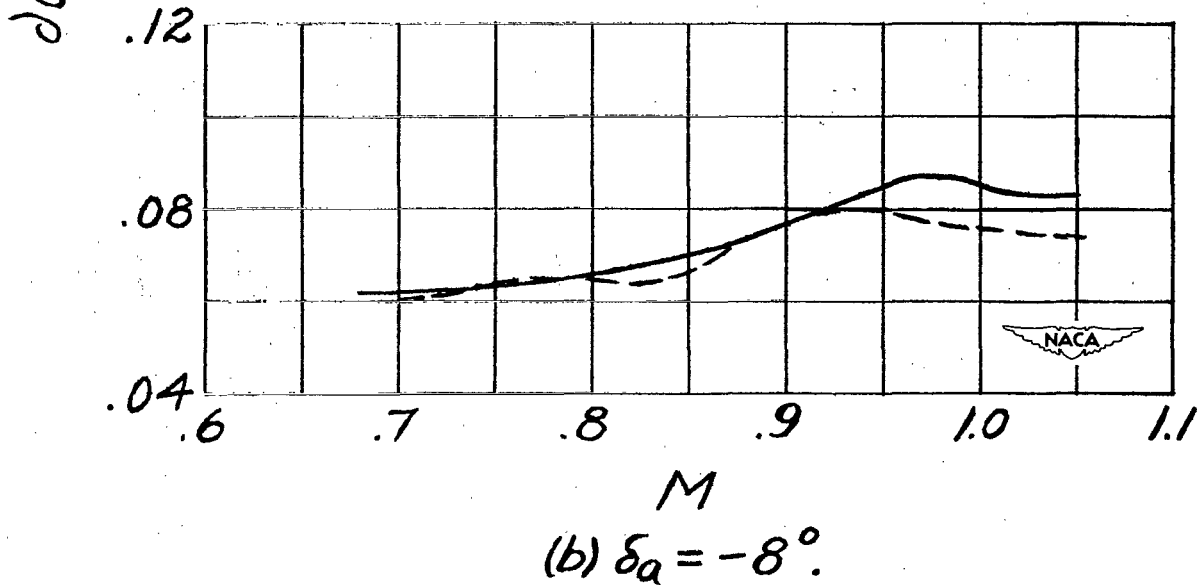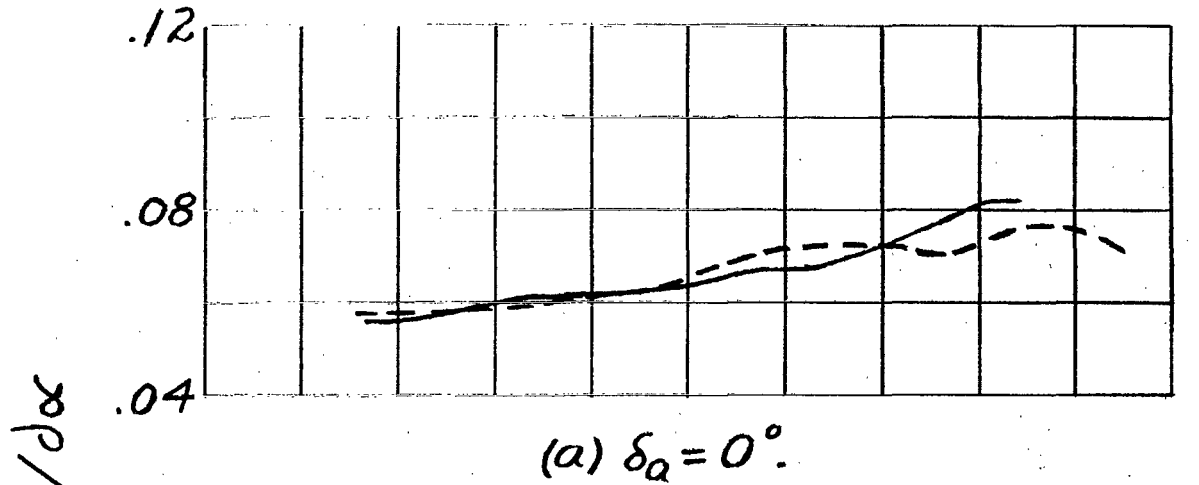
Figure 15.- Variation of normal-force-curve slope with Mach number at two ailavator deflections with speed brakes on. Results from reference 1 with speed brakes off shown for comparison.

(a) $\delta_a = 0°$.
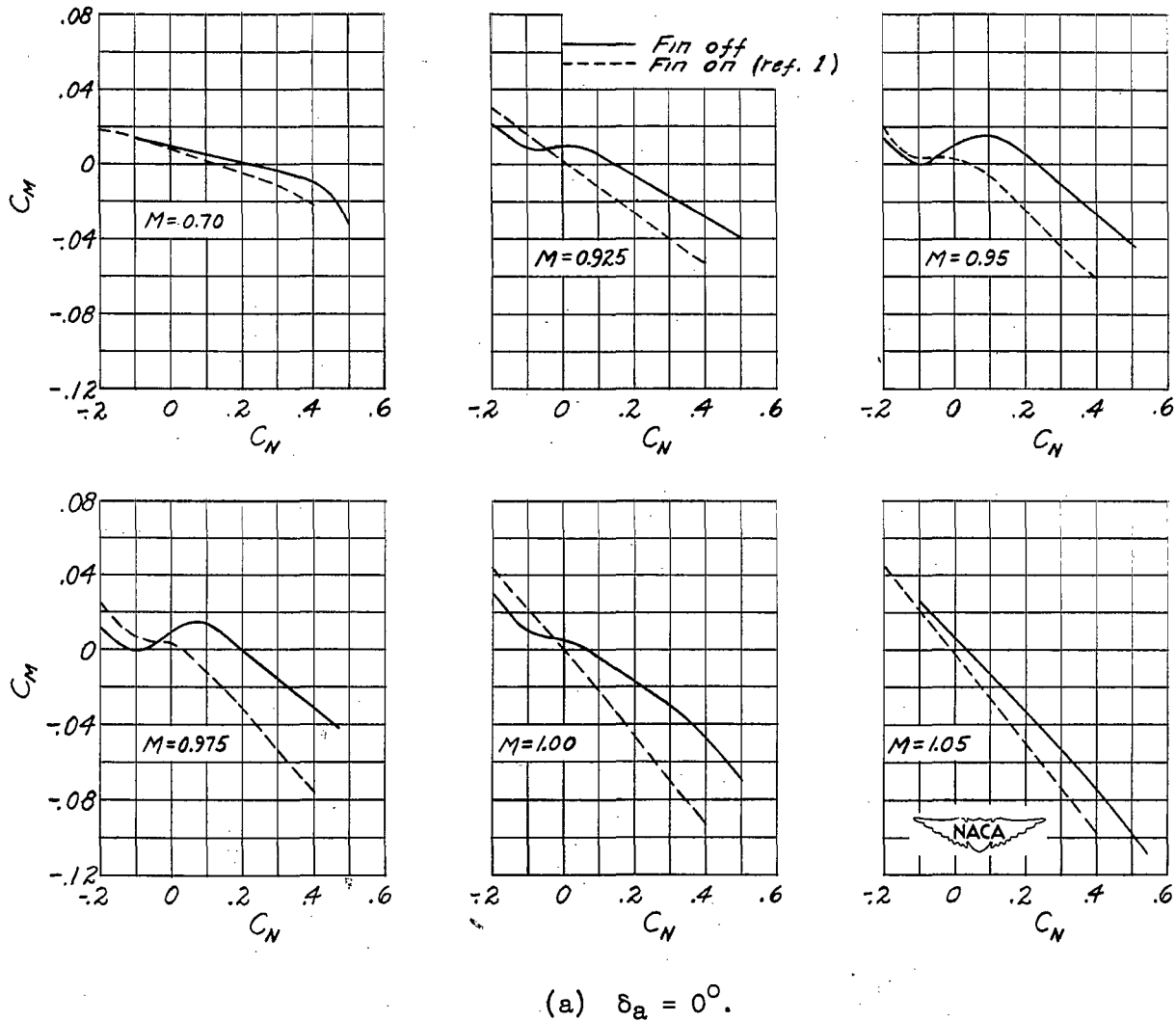
Figure 16.- Variation of pitching-moment coefficient with normal-force
coefficient at several Mach numbers for several ailavator deflections
with fin off. Results from reference 1 with fin on shown for
comparison.
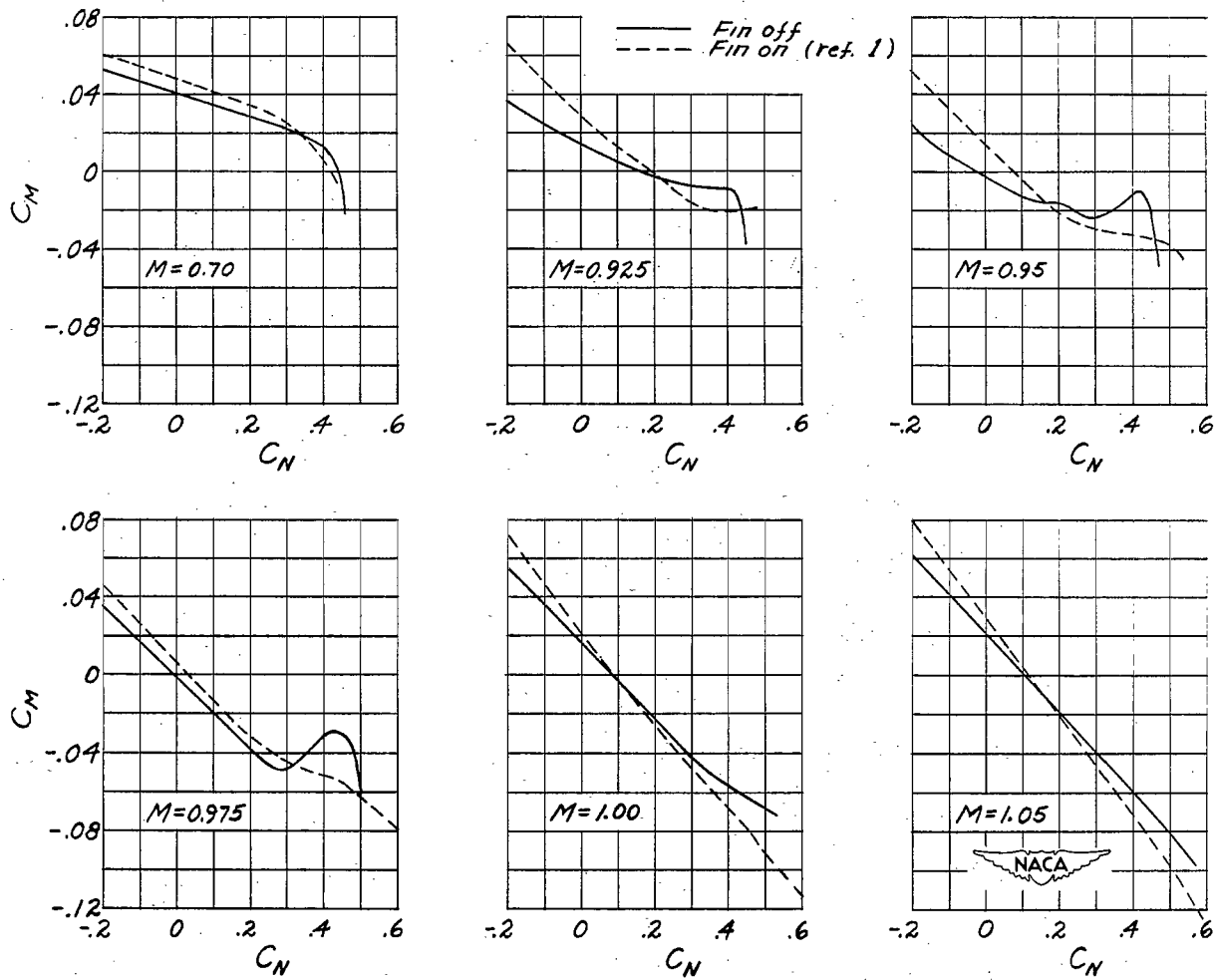
(b) $\delta_a = -4.9°$.

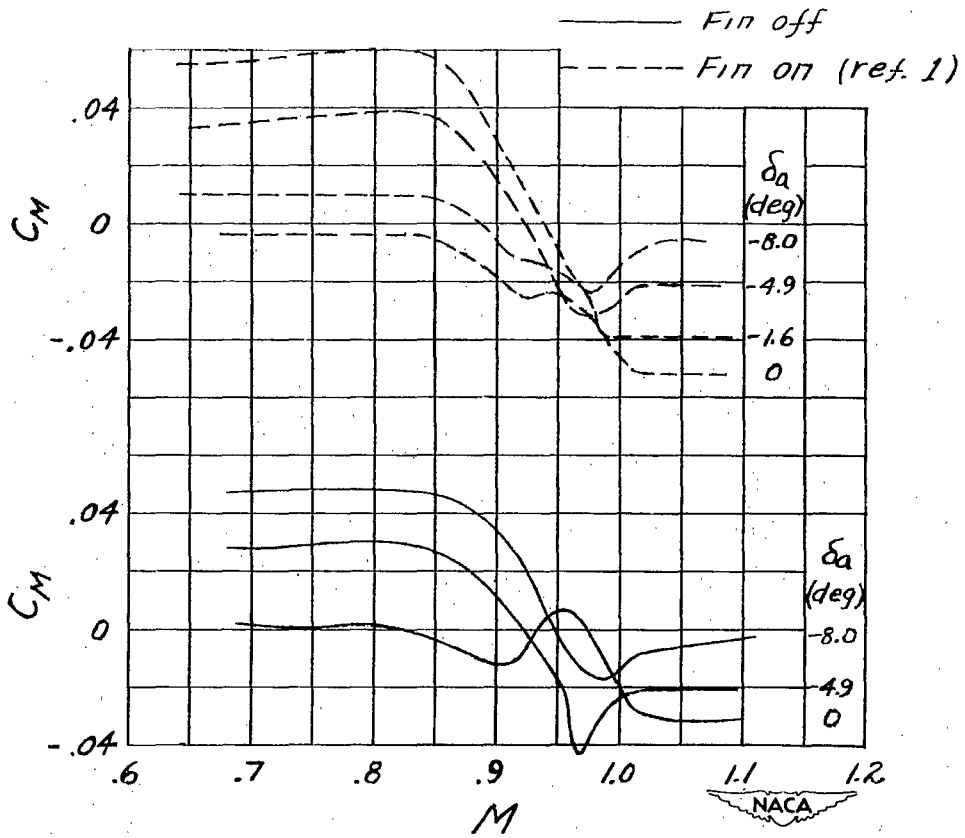Figure 16.- Continued.

Fin off
Fin on (ref. 1)

$M = 0.70$

$M = 0.925$

$M = 0.95$

$M = 0.975$

$M = 1.00$

$M = 1.05$
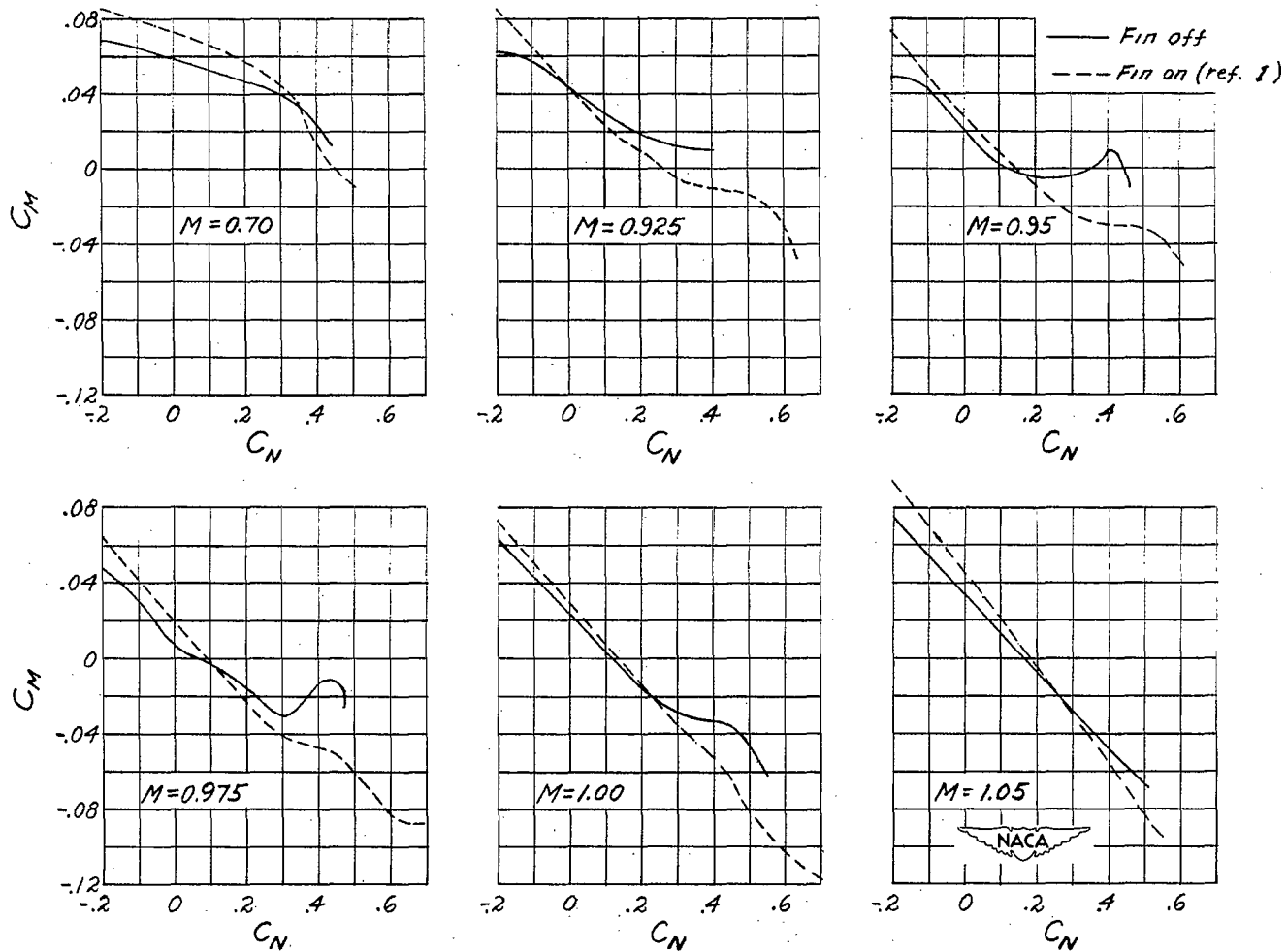
(c) $\delta_a = -8.0^\circ$.

Figure 16.- Concluded.
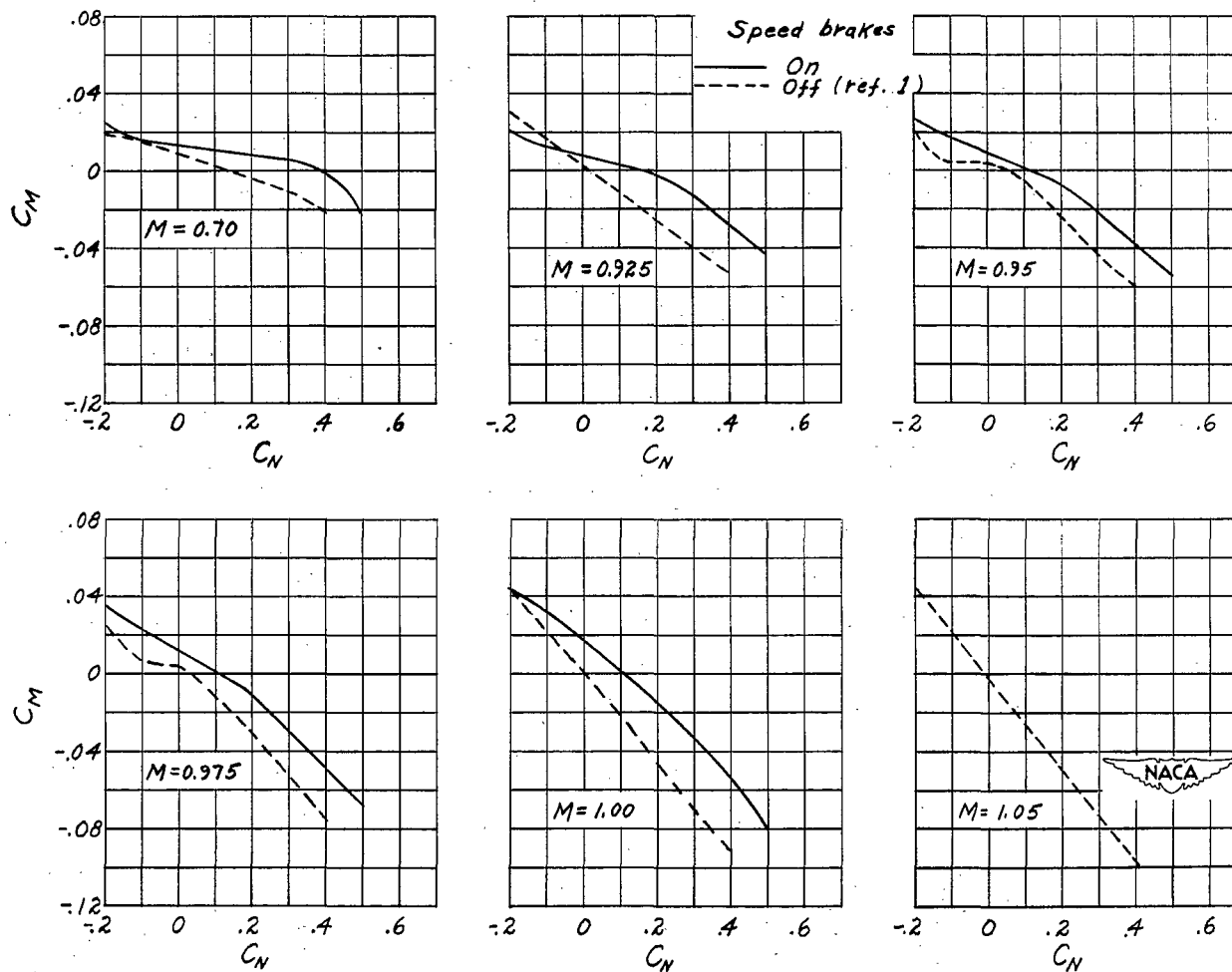
(a) $\delta_a = 0^\circ$.

Figure 17.- Variation of pitching-moment coefficient with normal-force
coefficient at several Mach numbers for two ailavator deflections
with speed brakes on. Results from reference 1 with speed brakes off
shown for comparison.
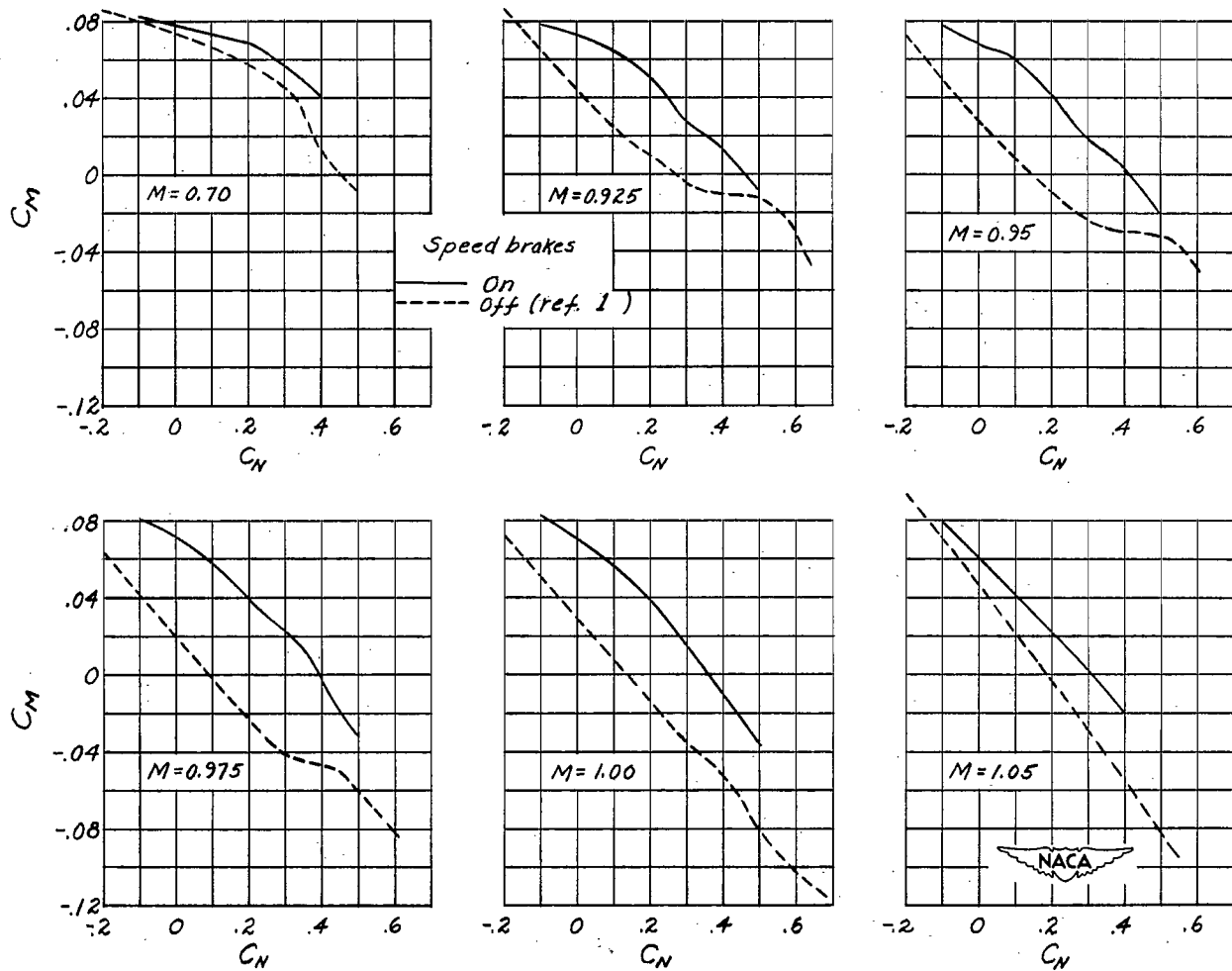
(b) $\delta_a = -8.0°$.

Figure 17.- Concluded.
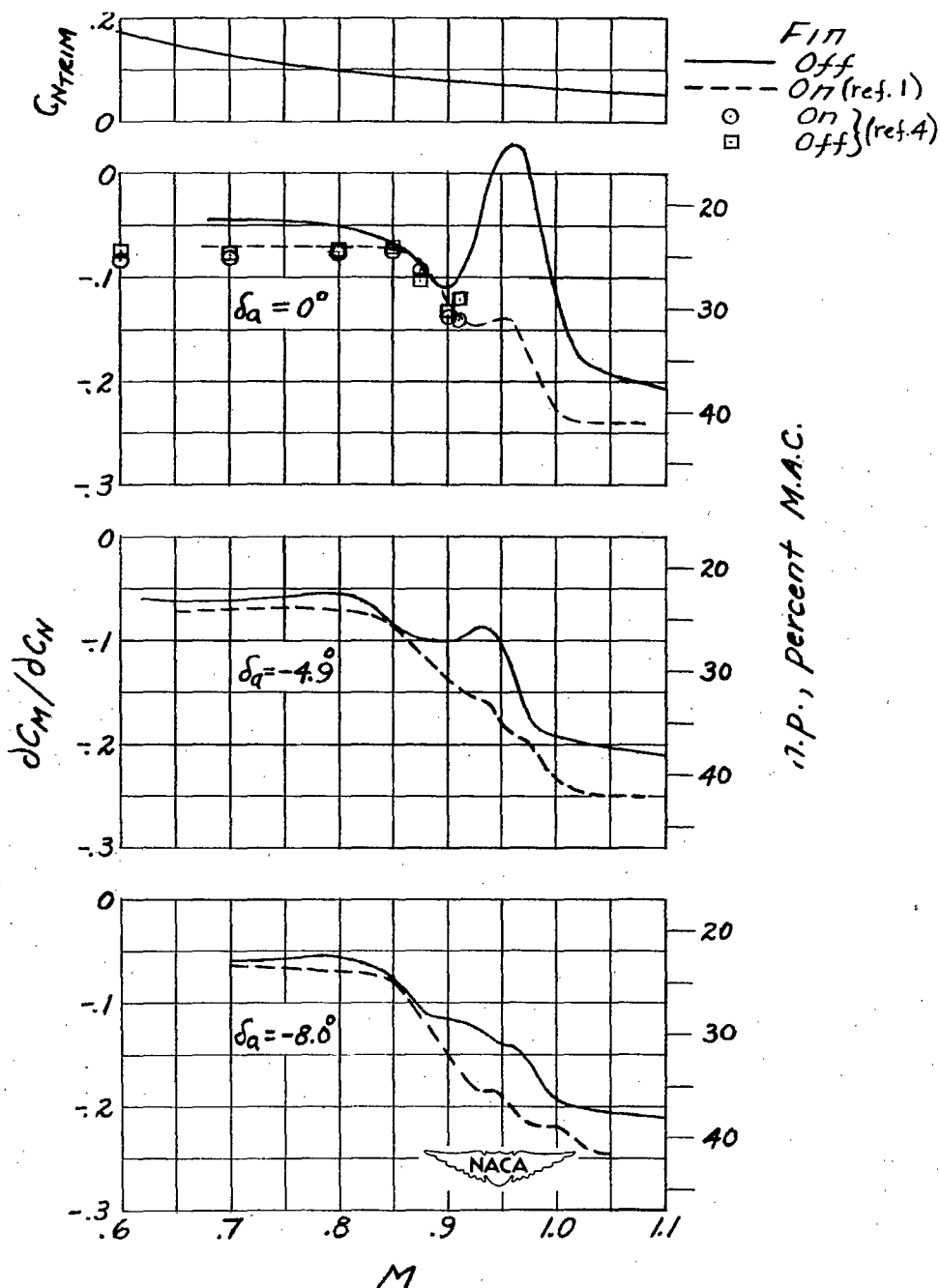
Figure 18.- Variation with Mach number of slope of pitching-moment

curve $\dfrac{\partial C_M}{\partial C_N}$ for several ailavator deflections with fin off. Results

from references 1 and 4 shown for comparison. Normal-force coeffi-
cient for level flight at 30,000 feet with wing loading of 28 also
shown.
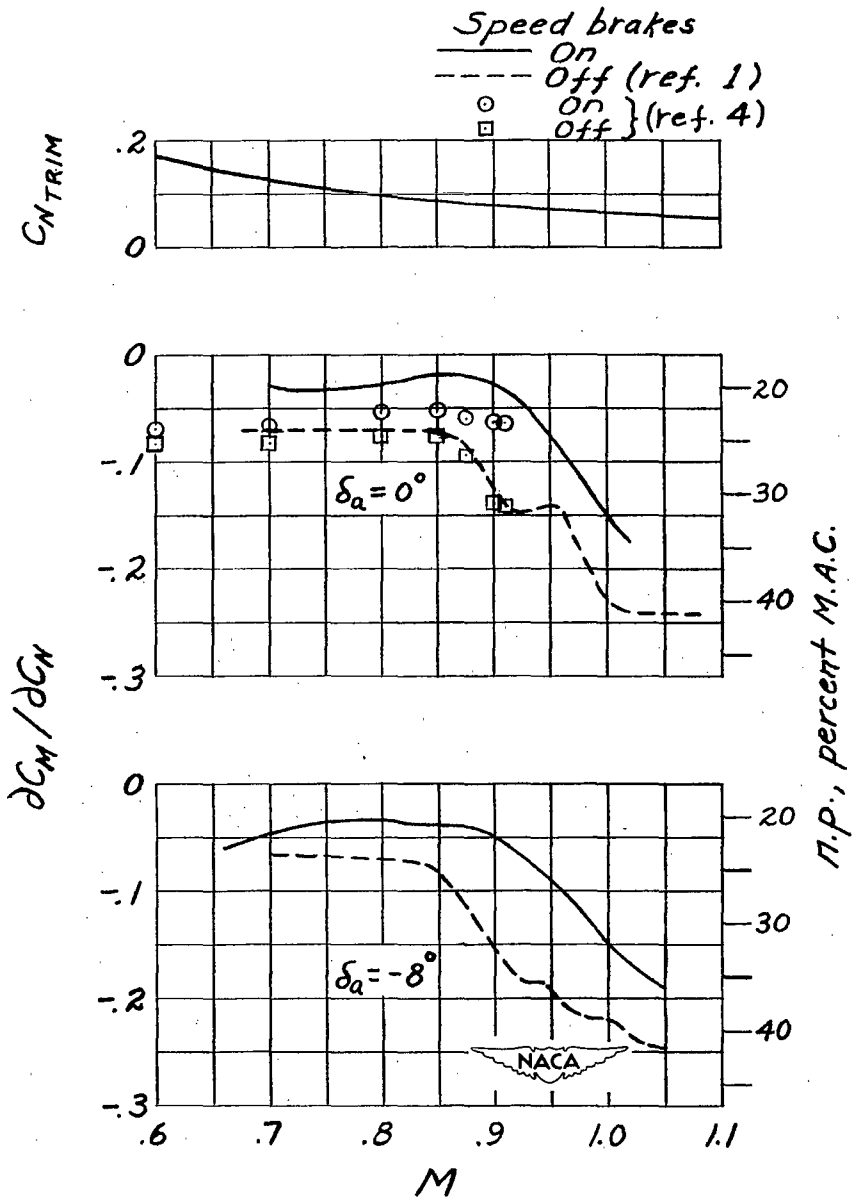
Figure 19.- Variation with Mach number of slope of pitching-moment curve $\frac{\partial C_M}{\partial C_N}$ for two ailavator deflections with speed brakes on. Results from references 1 and 4 shown for comparison. Normal-force coefficient for level flight at 30,000 feet with wing loading of 28 also shown.
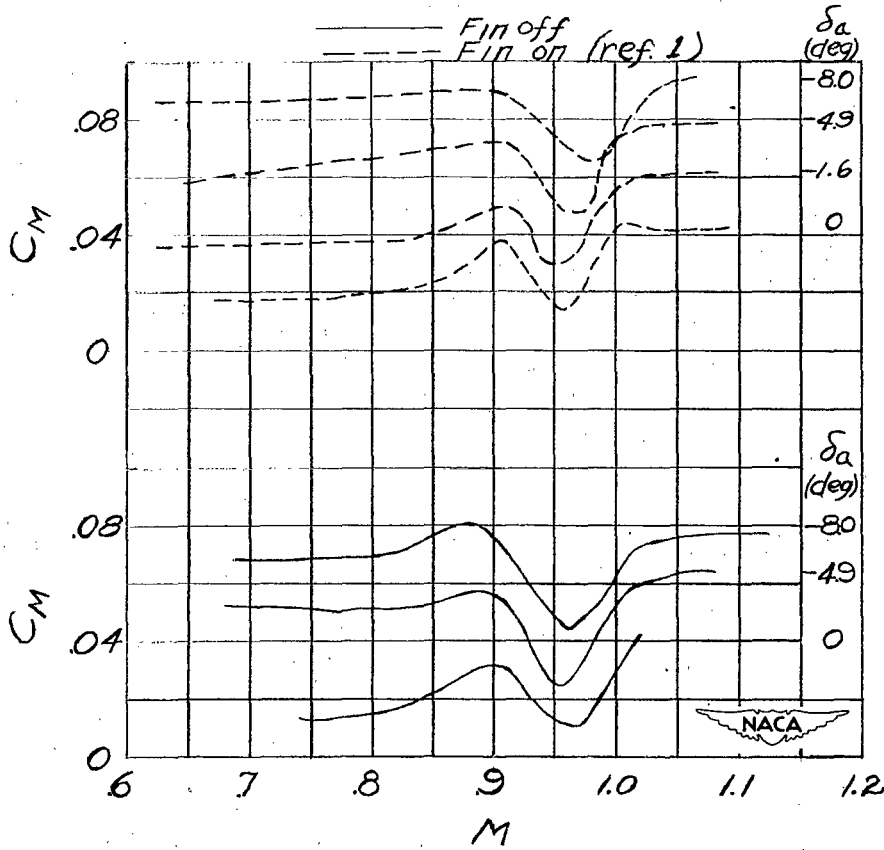
(a) $C_N = -0.2$.

Figure 20.- Variation of pitching-moment coefficient with Mach number
at several ailavator deflections for several normal-force coeffi-
cients with fin off. Results from reference 1 with fin on shown for
comparison.
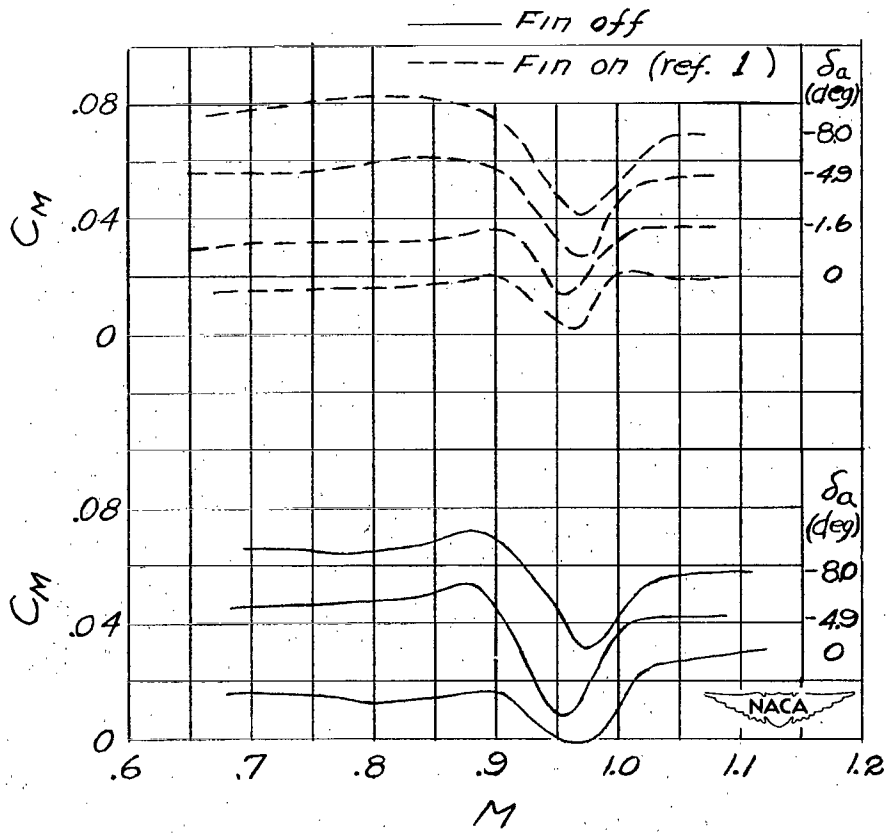
(b) $C_N = -0.1$.

Figure 20.- Continued.
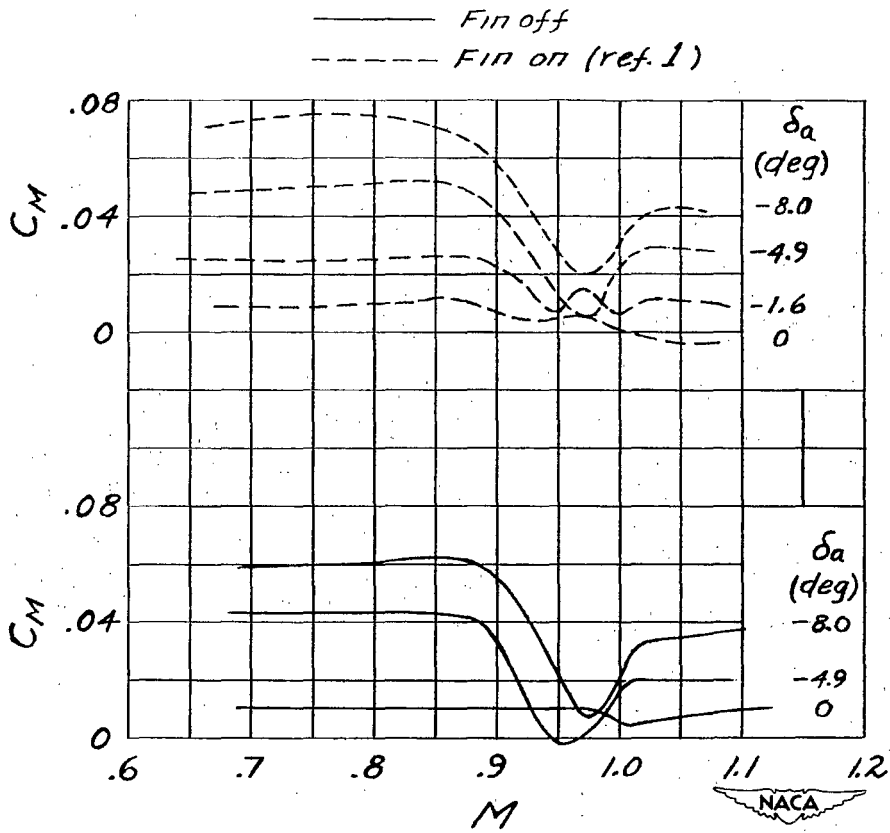
(c) $C_N = 0$.

Figure 20.- Continued.
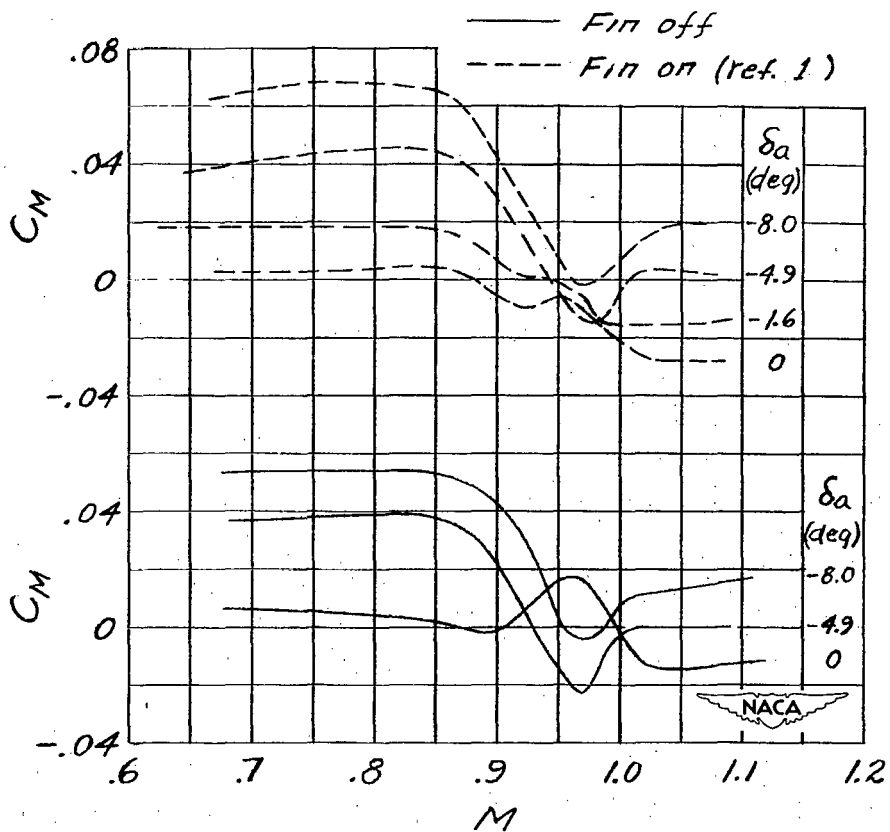
(d) $C_N = 0.1$.

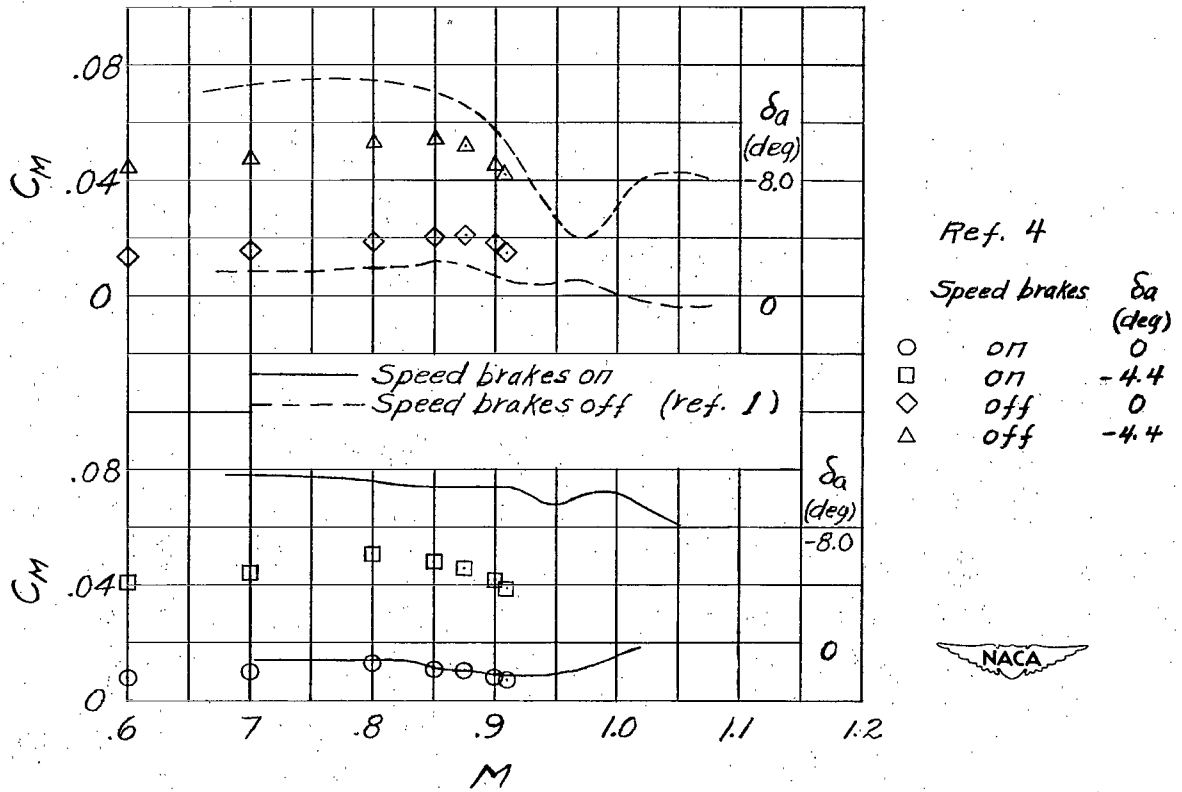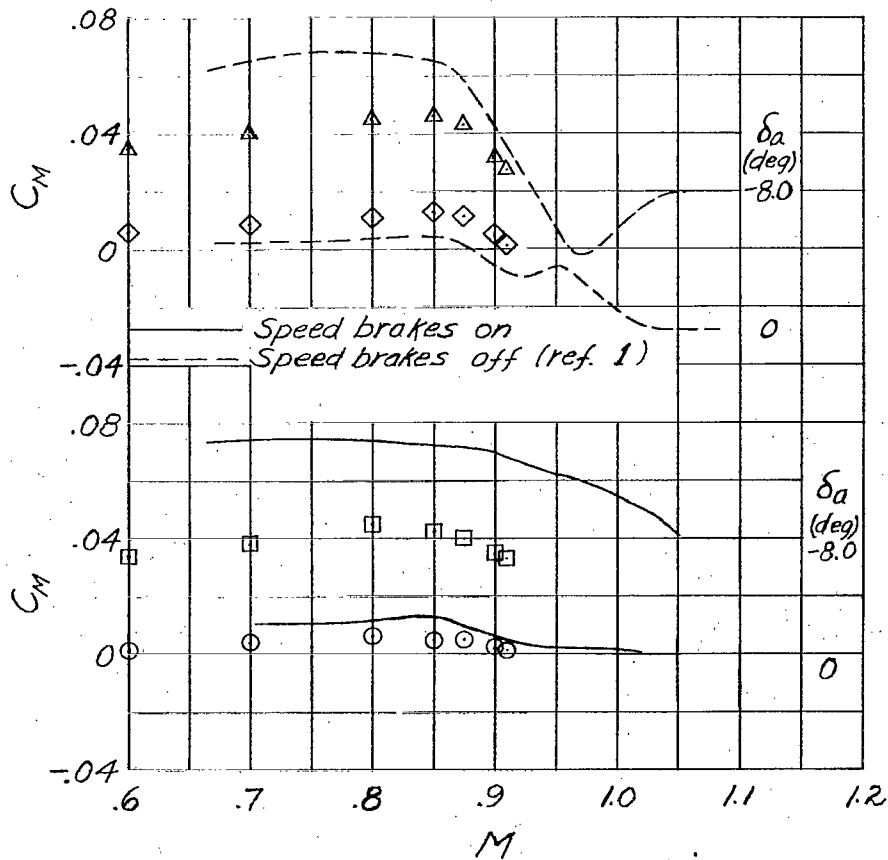Figure 20.- Continued.

(e) $C_N = 0.2$.

Figure 20.- Continued.
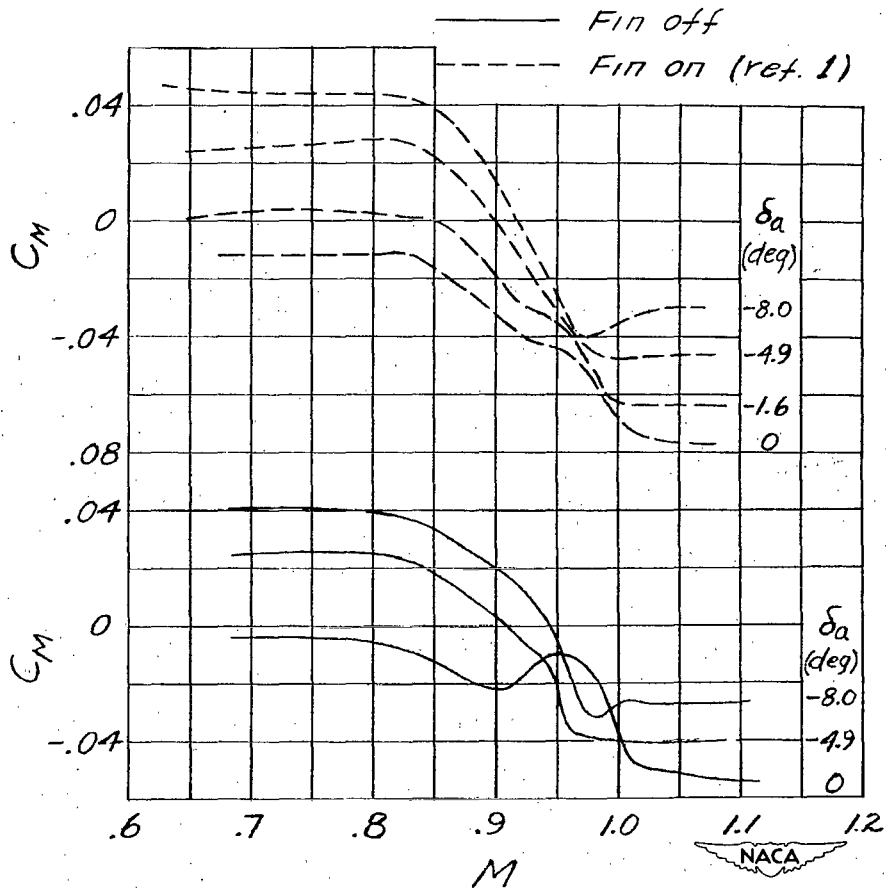
(f) C_N = 0.3.

Figure 20.- Concluded.
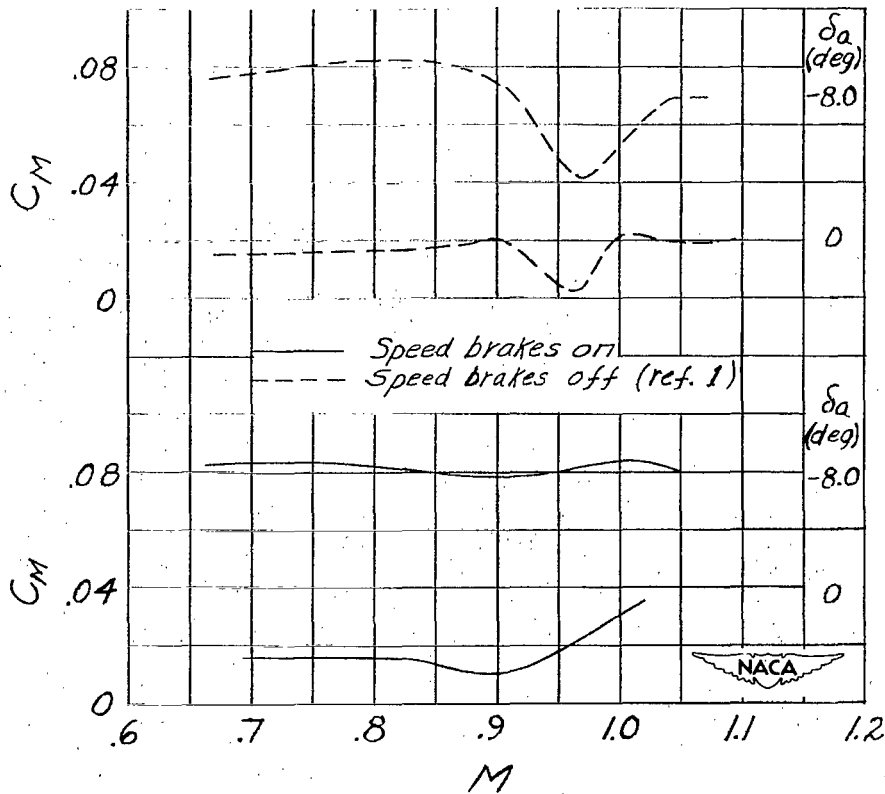
(a) $C_N = -0.1$.

Figure 21.- Variation of pitching-moment coefficient with Mach number
    at two ailavator deflections for several normal-force coefficients
    with speed brakes on. Results from reference 1 with speed brakes
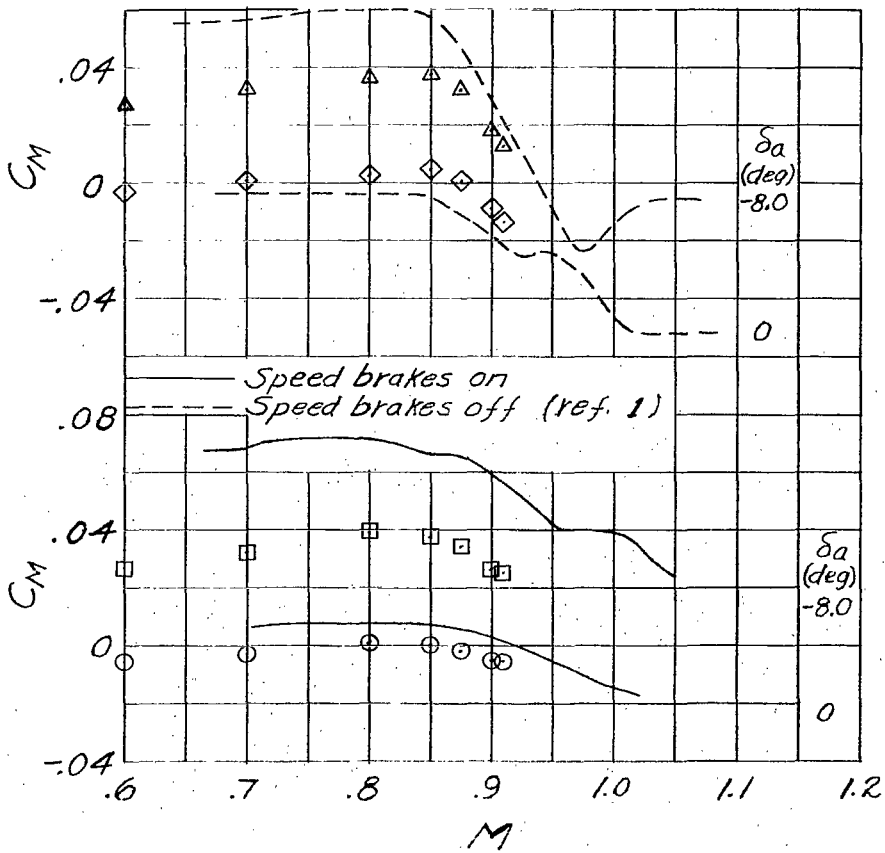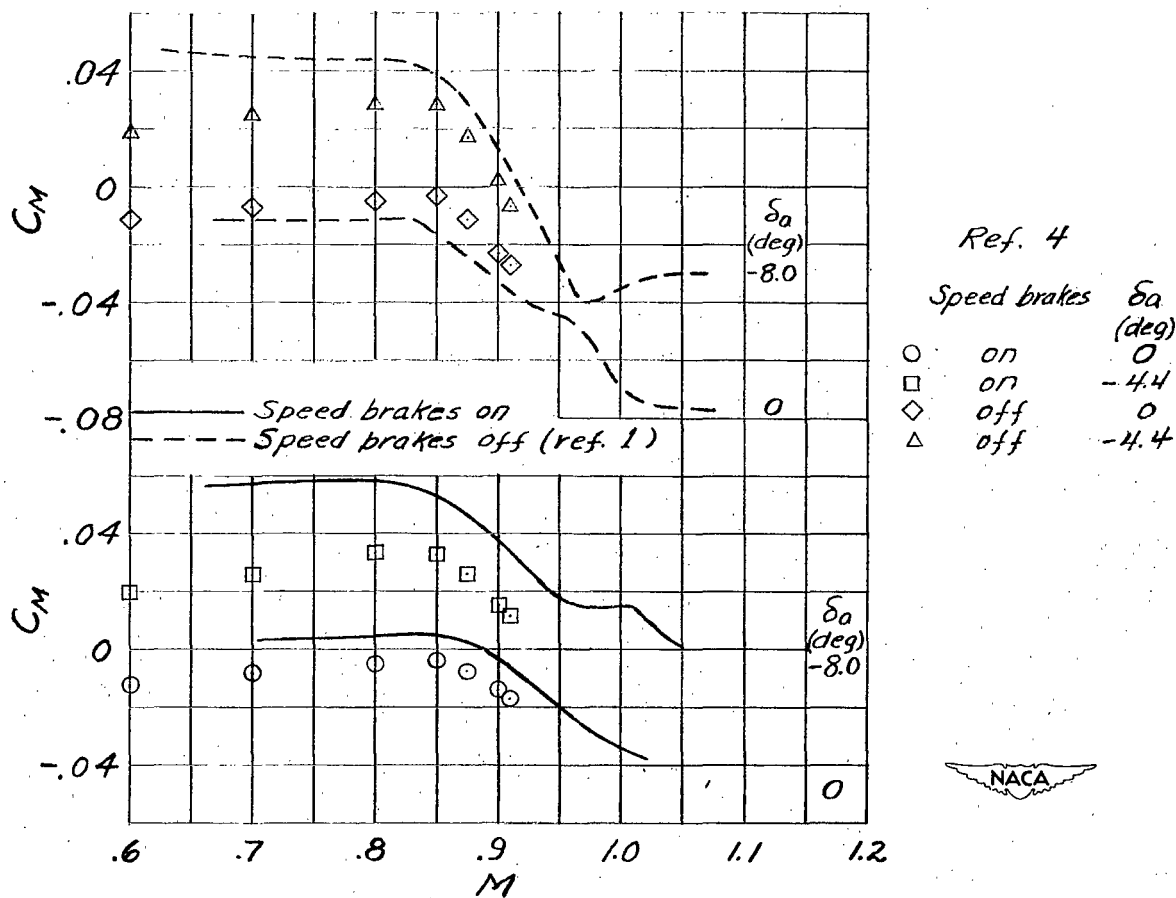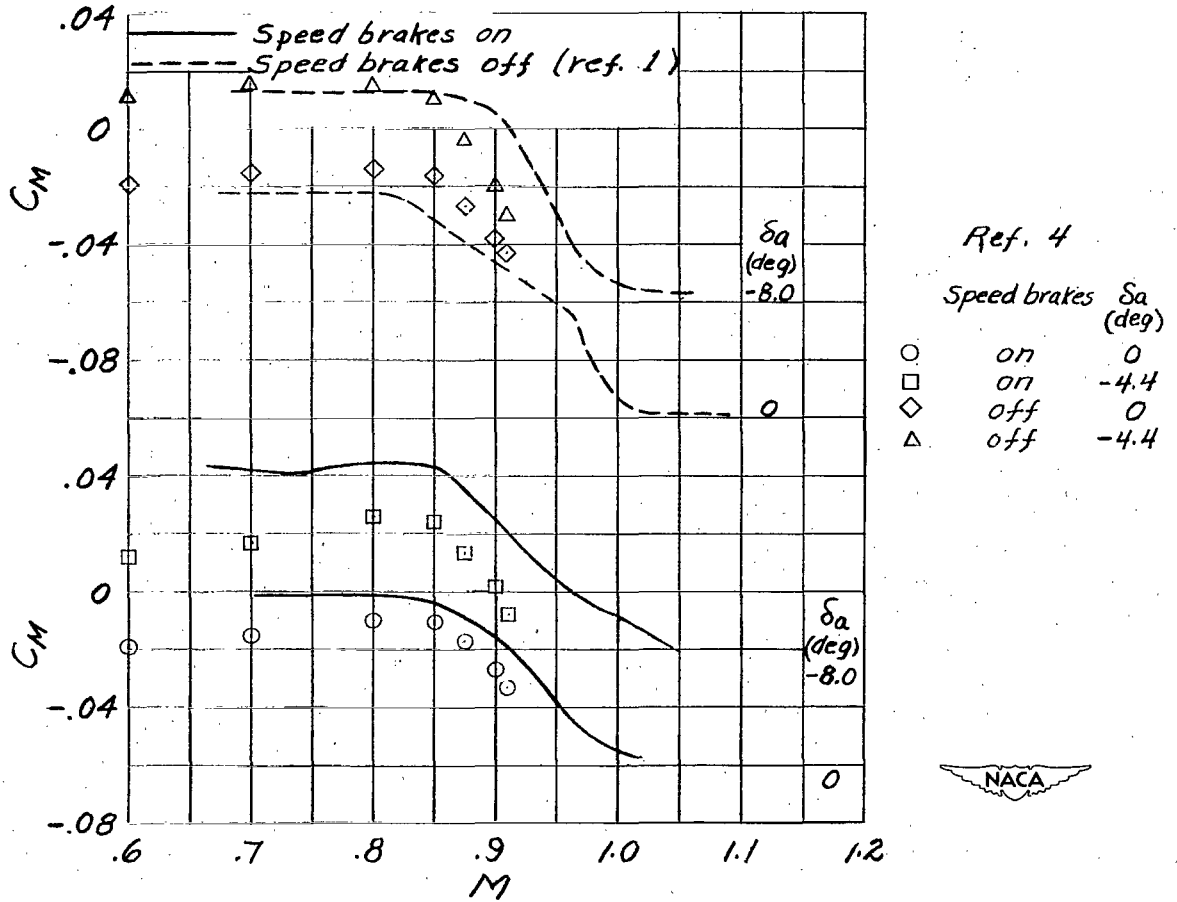   off shown for comparison.

δ_a (deg)

-8.0

0

——— Speed brakes on
— — — Speed brakes off (ref. 1)

δ_a (deg)

-8.0

0

.6   7   .8   .9   1.0   1.1   1.2

M

Ref. 4

Speed brakes	δ_a (deg)
on	0
on	-4.4
off	0
off	-4.4

(b) $C_N = 0$.

Figure 21.- Continued.

(c) $C_N = 0.1$.

Figure 21.- Continued.

(d) $C_N = 0.2$.

Figure 21.- Continued.

(e) $C_N = 0.3$.

Figure 21.- Continued.

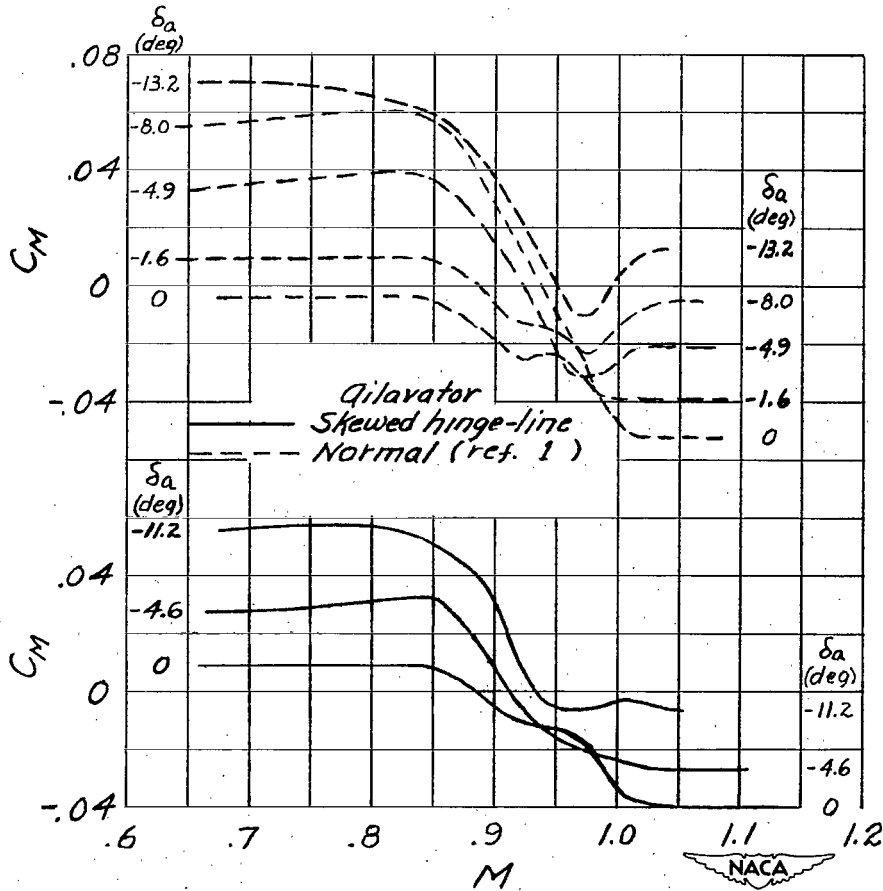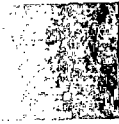(f) $C_N = 0.4$.

Figure 21.- Concluded.

Figure 22.- Variation of pitching-moment coefficient with Mach number at several deflections of ailavator having highly sweptback hinge line at a normal-force coefficient of 0.2. Results from reference 1 with normal ailavators shown for comparison.